

Forecasting range shifts of a dioecious plant species under climate change

Jacob K. Moutouama  *¹, Aldo Compagnoni  ², and Tom E.X. Miller  ¹

¹Program in Ecology and Evolutionary
Biology, Department of BioSciences, Rice University, Houston, Texas, USA

²Institute
of Biology, Martin Luther University Halle-Wittenberg, Halle, Germany; and
German Centre for Integrative Biodiversity Research (iDiv), Leipzig, Germany

*Corresponding author: jmoutouama@gmail.com

¹ Abstract

² Global warming has triggered an urgent need for predicting the reorganization of Earth's
³ biodiversity. Currently, the vast majority of models used to forecast population viability
⁴ and range shifts in response to climate change ignore the complication of sex structure, and
⁵ thus the potential for females and males to differ in their sensitivity to climate drivers. We
⁶ developed demographic models of range limitation, parameterized from geographically
⁷ distributed common garden experiments, with females and males of a dioecious grass species
⁸ (*Poa arachnifera*) throughout and beyond its range in the south-central U.S. Female-dominant
⁹ and two-sex model versions both predict that climate change will alter population viability and
¹⁰ will induce a poleward niche shift beyond current northern limits. However, the magnitude of
¹¹ niche shift was underestimated by the female-dominant model, because females have broader
¹² temperature tolerance than males and become mate-limited under female-biased sex ratios.
¹³ Our result illustrate how explicit accounting for both sexes could enhance population viability
¹⁴ forecasts and conservation planning for dioecious species in response to climate change.

¹⁵ **Keywords:** demography, forecasting, global warming, matrix projection model, population
¹⁶ dynamics, sex ratio, range limits

¹⁷ Introduction

¹⁸ Rising temperatures and extreme drought events associated with global climate change are
¹⁹ leading to increased concern about how species will become redistributed across the globe
²⁰ under future climate conditions (Bertrand et al., 2011; Gamelon et al., 2017; Smith et al., 2024).
²¹ Species' range limits, when not driven by dispersal limitation, should generally reflect the limits
²² of the ecological niche (Lee-Yaw et al., 2016). Niches and geographic ranges are often limited
²³ by climatic factors including temperature and precipitation (Sexton et al., 2009). Therefore,
²⁴ any substantial changes in the magnitude of these climatic factors could impact population
²⁵ viability, with implications for range expansions or contractions based on which regions of
²⁶ a species' range become more or less suitable (Davis and Shaw, 2001; Pease et al., 1989).

²⁷ Forecasting range shifts for dioecious species (most animals and ca. 7% of plant species)
²⁸ is complicated by the potential for sexual niche differentiation, i.e. distinct responses of
²⁹ females and males to shared climate drivers (Hultine et al., 2016; Morrison et al., 2016; Pottier
³⁰ et al., 2021; Tognetti, 2012). For instance, the lower cost of reproduction for one sex (male
³¹ or female) may allow that sex to invest its energy toward other functions that result in
³² higher growth rates, greater clonality, or even improved survival rates compared to the other
³³ sex, leading to sexual niche differentiation (Bruijning et al., 2017). Accounting for sexual niche
³⁴ differentiation is a long-standing challenge in accurately predicting which sex will successfully
³⁵ track environmental change and how this will impact population viability and range shifts
³⁶ (Gissi et al., 2023; Jones et al., 1999). Populations in which males are rare under current climatic
³⁷ conditions could experience low reproductive success due to sperm or pollen limitation that
³⁸ may lead to population decline in response to climate change that disproportionately favors
³⁹ females (Eberhart-Phillips et al., 2017). In contrast, climate change could expand male habitat
⁴⁰ suitability (e.g. upslope movement), which might increase seed set for mate-limited females
⁴¹ and favor range expansion (Petry et al., 2016). Across dioecious plants, for example, studies
⁴² suggest that future climate change toward hotter and drier conditions may favor male-biased
⁴³ sex ratios (Field et al., 2013; Hultine et al., 2016). Although the response of species to climate
⁴⁴ warming is an urgent and active area of research, few studies have disentangled the interaction
⁴⁵ between sex and climate drivers to understand their combined effects on population dynamics
⁴⁶ and range shifts, despite calls for such an approach (Gissi et al., 2023; Hultine et al., 2016).

⁴⁷ The vast majority of theory and models in population biology, including those used
⁴⁸ to forecast biodiversity responses to climate change, ignore the complication of sex structure
⁴⁹ (but see Ellis et al., 2017; Gissi et al., 2024; Pottier et al., 2021). Traditional approaches instead
⁵⁰ focus exclusively on females, assuming that males are in sufficient supply as to never limit
⁵¹ female fertility. In contrast, "two-sex" models are required to fully account for demographic

52 differences between females and males and sex-specific responses to shared climate drivers
53 (Gerber and White, 2014; Miller et al., 2011). Sex differences in maturation, reproduction,
54 and mortality schedules can generate skew in the operational sex ratio (OSR; sex ratio of
55 individuals available for mating) even if the birth sex ratio is 1:1 (Eberhart-Phillips et al., 2017;
56 Shelton, 2010). Climate and other environmental drivers can therefore influence the OSR
57 via their influence on sex-specific demographic rates. In a two-sex framework, demographic
58 rates both influence and respond to the OSR in a feedback loop that makes two-sex models
59 inherently nonlinear and more data-hungry than corresponding female-dominant models.
60 Given the additional complexity and data needs, forecasts of range dynamics for dioecious
61 species under future climate change that explicitly account for females, males, and their
62 inter-dependence are limited (Lynch et al., 2014; Petry et al., 2016).

63 Tracking the impact of climate change on population viability (λ) and distributional
64 limits of dioecious taxa depends on our ability to build mechanistic models that take into
65 account the spatial and temporal context of sex specific response to climate change, while
66 accounting for sources of uncertainty (Davis and Shaw, 2001; Evans et al., 2016). Structured
67 population models built from demographic data collected from geographically distributed
68 observations or common garden experiments provide several advantages for studying
69 the impact of climate change on species' range shifts (Merow et al., 2017; Schultz et al.,
70 2022; Schwinning et al., 2022). First, demographic models link individual-level life history
71 events (mortality, development, and regeneration) to population demography, allowing the
72 investigation of factors explaining vital rate responses to environmental drivers (Dahlgren
73 et al., 2016; Ehrlén and Morris, 2015; Louthan et al., 2022). Second, demographic models
74 have a natural interface with statistical estimation of individual-level vital rates that provide
75 quantitative measures of uncertainty and isolate different sources of variation, features that
76 can be propagated to population-level predictions (Elderd and Miller, 2016; Ellner et al.,
77 2022). Finally, structured demographic models can be used to identify which aspects of
78 climate are the most important drivers of population dynamics. For example, Life Table
79 Response Experiments (LTRE) built from structured models have become widely used to
80 understand the relative importance of covariates in explaining variation in population growth
81 rate (Czachura and Miller, 2020; Ellner et al., 2016; Hernández et al., 2023).

82 In this study, we combined geographically-distributed common garden experiments,
83 hierarchical Bayesian statistical modeling, two-sex population projection modeling, and climate
84 back-casting and forecasting to understand demographic responses to climate change and their
85 implications for past, present, and future range dynamics. Our work focused on the dioecious
86 plant Texas bluegrass (*Poa arachnifera*), which is distributed along environmental gradients
87 in the south-central U.S. corresponding to variation in temperature across latitude and

88 precipitation across longitude (Fig. S-1A). This region has experienced rapid climate warming
89 since 1900 and this is projected to continue through the end of the century (Fig. 1). Our
90 previous study showed that, despite evidence for differentiation of climatic niche between sexes,
91 the female niche mattered the most in driving longitudinal range limits of Texas bluegrass
92 (Miller and Compagnoni, 2022b). However, that study used a single proxy variable (longitude)
93 to represent environmental variation related to aridity and did not consider variation in
94 temperature, which is the much stronger dimension of forecasted climate change in this region
95 (Fig. S-3). Developing a rigorous forecast for the implications of future climate change requires
96 that we transition from implicit to explicit treatment of multiple climate drivers, as we do
97 here. Leveraging the power of Bayesian inference, we take a probabilistic view of past, present,
98 and future range limits by quantifying the probability of population viability ($Pr(\lambda \geq 1)$) in
99 relation to climate drivers of demography, an approach that fully accounts for uncertainty
100 arising from multiple sources of estimation and process error. Specifically, we asked:

- 101 1. What are the sex-specific vital rate responses to variation in temperature and precipitation
102 across the species' range?
- 103 2. How do sex-specific vital rates combine to determine the influence of climate variation
104 on population growth rate (λ)?
- 105 3. What is the impact of climate change on operational sex ratio throughout the range?
- 106 4. What are the likely historical and projected dynamics of the Texas bluegrass geographic
107 niche and how does accounting for sex structure modify these predictions?

108 Materials and methods

109 Study species and climate context

110 Texas bluegrass (*Poa arachnifera*) is a dioecious perennial, summer-dormant cool-season (C3)
111 grass that occurs in the south-central U.S. (Texas, Oklahoma, and southern Kansas) (Figure
112 1) (Hitchcock, 1971). Texas bluegrass grows between October and May, flowers in spring,
113 and goes dormant during the hot summer months of June to September (Kindiger, 2004).
114 Following this life history, we divided the calendar year into growing (October 1 - May
115 31) and dormant (June 1 - September 30) seasons in the analyses below. Biological sex is
116 genetically based and the birth (seed) sex ratio is 1:1 (Renganayaki et al., 2005). Females and
117 males are morphologically indistinguishable except for their inflorescences. Like all grasses,
118 this species is wind pollinated (Hitchcock, 1971) and most male-female pollen transfer occurs
119 within 10-15m (Compagnoni et al., 2017). Surveys of 22 natural populations throughout the

¹²⁰ species' distribution indicated that operational sex ratio (the female fraction of inflorescences)
¹²¹ ranged from 0.007 to 0.986 with a mean of 0.404 (Miller and Compagnoni, 2022b).

¹²² Latitudinal limits of the Texas bluegrass distribution span 7.74 °C to 16.94 °C of
¹²³ temperature during the dormant season and 24.38 °C to 28.80 °C during the dormant season.
¹²⁴ Longitudinal limits span 244.9 mm to 901.5 mm of precipitation during the growing season
¹²⁵ and 156.3 mm to 373.3 mm. This region has experienced *ca.* 0.5 °C of climate warming since
¹²⁶ 1900, with faster warming during the cool-season months ($0.0055^{\circ}\text{C}/\text{yr}$) than the hot summers
¹²⁷ ($0.0046^{\circ}\text{C}/\text{yr}$) (Fig. S-2). Future warming is projected to accelerate to $0.03 - 0.06^{\circ}\text{C}/\text{yr}$ by
¹²⁸ the end of the century depending on the season and forecast model. On the other hand,
¹²⁹ precipitation has increased over the past century for much of the region but is forecasted
¹³⁰ to decline back to early-20th century levels (Fig. S-2).

¹³¹ Common garden experiment

¹³² Experimental design

¹³³ We conducted a range-wide common garden experiment to quantify sex-specific demographic
¹³⁴ responses to climate variation. Details of the experimental design are provided in Miller
¹³⁵ and Compagnoni (2022b); we provide a brief overview here. The experiment was installed
¹³⁶ at 14 sites throughout and, in some cases, beyond the natural range of Texas bluegrass that
¹³⁷ sampled a broad range of latitude and longitude (Figure 1A). At each site, we established
¹³⁸ 14 blocks. For each block we planted three female and three male individuals that were
¹³⁹ clonally propagated from females and males from eight natural source populations (Figure
¹⁴⁰ 1A); because sex is genetically-based, clones never deviated from their expected sex. The
¹⁴¹ experiment was established in November 2013 with a total of 588 female and 588 male plants,
¹⁴² and was censused in May of 2014, 2015, and 2016. At each census, we collected data on
¹⁴³ survival, size (number of tillers), and number of panicles (reproductive inflorescences). For
¹⁴⁴ the analyses that follow, we focus on the 2014-15 and 2015-16 transition years, since the start
¹⁴⁵ of the experiment did not include the full 2013-14 transition year.

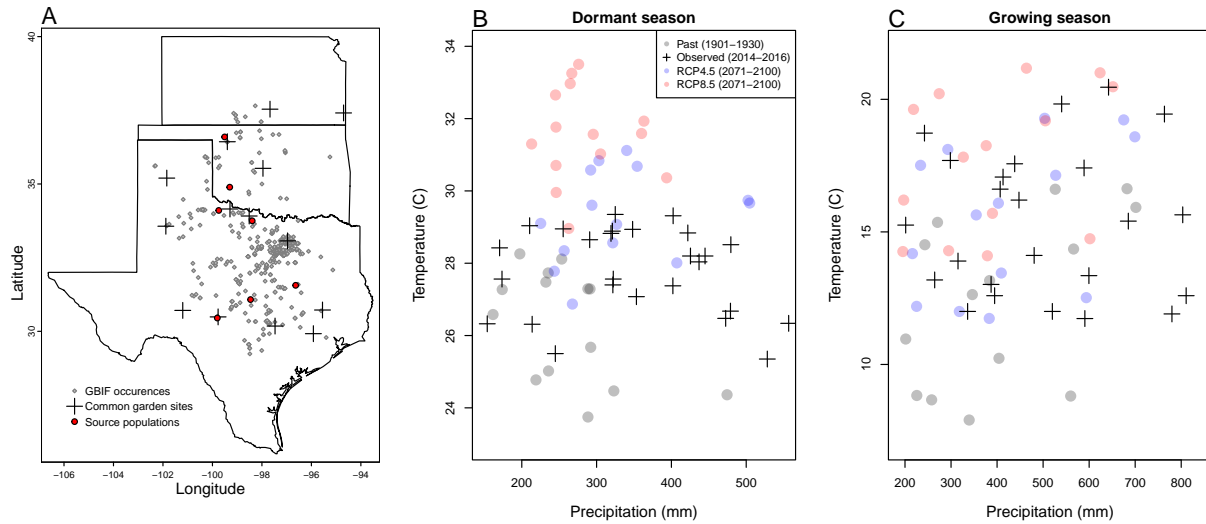


Figure 1: Experimental gardens and climate of the study region. **A:** Map of 14 experimental garden sites (crosses) in Texas, Oklahoma, and Kansas relative to GBIF occurrences of *Poa arachnifera* (gray points). Red points indicate source populations for plants used in the common garden experiment. **B,C:** Past, future, and observed climate space for growing and dormant seasons. Crosses show observed conditions for the sites and years of the common garden experiment. Gray points show historical (1901-1930) climate normals, and blue and red points show end-of-century (2071-2100) climate normals for RCP4.5 and RCP8.5 projections, respectively, from MIROC5.

146 Climatic data collection

147 We gathered downscaled monthly temperature and precipitation for each site from Chelsa
 148 (Karger et al., 2017) to describe observed climate conditions during our study period. These
 149 climate data were used as covariates in vital rate regressions. We aligned the climatic years
 150 to match demographic transition years (June 1 – May 31) and growing and dormant seasons
 151 within each year. To back-cast and forecast demographic responses to changes in climate
 152 throughout the study region, we also gathered projection data for three 30-year periods: “past”
 153 (1901-1930), “current” (1990-2019) and “future” (2070-2100). Data for future climatic periods
 154 were downloaded from four general circulation models (GCMs) selected from the Coupled
 155 Model Intercomparison Project Phase 5 (CMIP5): Model for Interdisciplinary Research on
 156 Climate (MIROC5), Australian Community Climate and Earth System Simulator (ACCESS1-3),
 157 Community Earth System Model (CESM1-BGC), Centro Euro-Mediterraneo sui Cambiamenti
 158 Climatici Climate Model (CMCC-CM). All the GCMs were also downloaded from Chelsa
 159 (Sanderson et al., 2015). We evaluated future climate projections from two scenarios of
 160 representative concentration pathways (RCPs): RCP4.5, an intermediate-to-pessimistic scenario
 161 assuming a radiative forcing amounting to 4.5 W m^{-2} by 2100, and RCP8.5, a pessimistic

162 emission scenario which projects a radiative forcing of 8.5 Wm^{-2} by 2100 (Schwalm et al.,
163 2020; Thomson et al., 2011).

164 Projection data for the three 30-year periods included warmer or colder conditions than ob-
165 served in our experiment, so extending our inferences to these conditions required some extrap-
166 olation. However, across all sites, both study years were 1–2°C warmer than their correspond-
167 ing “current” (1990–2019) temperature normals (Fig. S-3). Additionally, the 2014–15 growing
168 season was generally wetter and cooler across the study region than 2015–16 (Fig. S-3). Com-
169 bined, the geographic and inter-annual replication of the common garden experiment provided
170 good coverage of most past and future conditions throughout the study region (Fig. 1B,C).

171 **Sex-specific demographic responses to climatic variation across common garden sites**

172 We used individual-level measurements of survival, growth (change in number of tillers),
173 flowering, and number of panicles (conditional on flowering) to develop Bayesian mixed
174 effect models describing how each vital rate varies as a function of sex, size, and four climate
175 covariates (precipitation and temperature of growing and dormant season). These vital rate
176 models included main effects of size (the natural log of tiller number), sex, and seasonal
177 climate covariates (Supplementary Method S.2.1).

178 **Sex ratio responses to climatic variation across common garden sites**

179 We also used the experimental data to investigate how climatic variation across the range
180 influenced sex ratio and operational sex ratio of the common garden populations. To do so,
181 we developed two Bayesian linear models using data collected during three years. Each model
182 had OSR or SR as response variable and a climate variable (temperature and precipitation
183 of the growing season and dormant season) as predictor (Supplementary Method S.2.2).

184 **Model-fitting procedures**

185 All models were fit using Stan (Stan Development Team, 2023) in R 4.3.1 (R Core Team,
186 2023). We centered and standardized all climatic predictors to mean zero, variance one, which
187 facilitated model convergence. We ran three chains for 1000 samples for warmup and 4000
188 for sampling, with a thinning rate of 3. We assessed the quality of the models using posterior
189 predictive checks (Piironen and Vehtari, 2017) (Fig. S-4).

190 **Two-sex and female-dominant matrix projection models**

191 We used the climate-dependent vital rate regressions estimated above, combined with
 192 additional data sources, to build female-dominant and two-sex versions of a climate-explicit
 193 matrix projection model (MPMs) structured by the discrete state variables size (number
 194 of tillers) and sex. The female-dominant and two-sex versions of the model both allow
 195 for sex-specific response to climate and differ only in the feedback between operational
 196 sex ratio and seed fertilization. For clarity of presentation we do not explicitly include
 197 climate-dependence in the notation below, but the following model was evaluated over
 198 variation in seasonal temperature and precipitation.

199 Let $F_{x,t}$ and $M_{x,t}$ be the number of female and male plants of size x in year t , where
 200 $x \in [1, \dots, U]$. The minimum possible size is one tiller and U is the 95th percentile of observed
 201 maximum size (35 tillers). Let F_t^R and M_t^R be new female and male recruits in year t , which
 202 we treat as distinct from the rest of the size distribution because we assume they do not
 203 reproduce in their first year, consistent with our observations. For a pre-breeding census,
 204 the expected numbers of recruits in year $t+1$ is given by:

$$205 F_{t+1}^R = \sum_1^U [p^F(x) \cdot c^F(x) \cdot d \cdot v(\mathbf{F}_t, \mathbf{M}_t) \cdot m \cdot \rho] F_{x,t} \quad (1)$$

$$206 M_{t+1}^R = \sum_1^U [p^F(x) \cdot c^F(x) \cdot d \cdot v(\mathbf{F}_t, \mathbf{M}_t) \cdot m \cdot (1-\rho)] F_{x,t} \quad (2)$$

207 where p^F and c^F are flowering probability and panicle production for females of size x , d
 208 is the number of seeds per female panicle, v is the probability that a seed is fertilized, m is
 209 the probability that a fertilized seed germinates, and ρ is the primary sex ratio (proportion
 210 of recruits that are female), which we assume to be 0.5 (Miller and Compagnoni, 2022b).

211 In the two-sex model, seed fertilization is a function of population structure, allowing for
 212 feedback between vital rates and operational sex ratio (OSR). In the context of the model, OSR
 213 is defined as the fraction of panicles that are female and is derived from the $U \times 1$ vectors
 214 \mathbf{F}_t and \mathbf{M}_t :

$$215 v(\mathbf{F}_t, \mathbf{M}_t) = v_0 * \left[1 - \left(\frac{\sum_1^U p^F(x, z) c^F(x, z) F_{x,t}}{\sum_1^U p^F(x, z) c^F(x, z) F_{x,t} + p^M(x, z) c^M(x, z) M_{x,t}} \right)^\alpha \right] \quad (3)$$

216 The summations tally the total number of female and male panicles over the size distribution,
 217 giving the fraction of total panicles that are female. We focus on the female fraction of
 218 panicles and not female fraction of reproductive individuals because panicle number can vary
 219 widely depending on size; we assume that few males with many panicles vs. many males

220 with few panicles are interchangeable pollination environments. Eq. 3 has the properties
 221 that seed fertilization is maximized at v_0 as OSR approaches 100% male, goes to zero as OSR
 222 approaches 100% female, and parameter α controls how female seed viability declines as male
 223 panicles become rare. We estimated these parameters using data from a sex ratio manipulation
 224 experiment, conducted in the center of the range, in which seed fertilization was measured
 225 in plots of varying OSR; this experiment is described elsewhere (Compagnoni et al., 2017) and
 226 is summarized in Supplementary Method S.2.3. This experiment also provided estimates for
 227 seed number per panicle (d) and germination rate (m). Lacking data on climate-dependence,
 228 we assume that seed fertilization, seed number, and germination rate do not vary with climate.
 229

The dynamics of the size-structured component of the population are given by:

$$F_{y,t+1} = [\sigma \cdot g^F(y, x=1)] F_t^R + \sum_L^U [s^F(x) \cdot g^F(y, x)] F_{x,t} \quad (4)$$

$$M_{y,t+1} = [\sigma \cdot g^M(y, x=1)] M_t^R + \sum_L^U [s^M(x) \cdot g^M(y, x)] M_{x,t} \quad (5)$$

232 The first terms indicate recruits that survived their first year and enter the size distribution
 233 of established plants. We estimated the seedling survival probability σ using demographic
 234 data from the congeneric species *Poa autumnalis* in east Texas (T.E.X. Miller and J.A. Rudgers,
 235 *unpublished data*), and we assume that σ is the same across sexes and climatic variables. We did
 236 this because we had little information on the early life cycle transitions of greenhouse-raised
 237 transplants. We used $g(y, x=1)$ (the future size distribution of one-tiller plants from the
 238 transplant experiment) to give the probability that a surviving recruit reaches size y . The
 239 second component of the equations indicates survival and size transition of established
 240 plants from the previous year, where s and g give the probabilities of surviving at size x and
 241 growing from sizes x to y , respectively, and superscripts indicate that these functions may
 242 be unique to females (F) and males (M).

243 The model described above yields a $2(U+1) \times 2(U+1)$ transition matrix. We estimated
 244 the population growth rate λ of the female dominant model as the leading eigenvalue of
 245 the transition matrix. Since the two-sex MPM is nonlinear (matrix elements affect and are
 246 affected by population structure) we estimated λ and stable sex ratio (female fraction of all
 247 individuals) and operational sex ratio (female fraction of panicles) by numerical simulation.
 248 Since all parameters were estimated using MCMC sampling, we were able to propagate the
 249 uncertainty in our estimates of the vital rate parameters to uncertainty in λ . Furthermore,
 250 by sampling over distributions associated with site, block, and source population variance
 251 terms, we are able to incorporate process error into the total uncertainty in λ , in addition
 252 to the uncertainty that arises from imperfect knowledge of the parameter values. For example,

253 sampling over site and block variances accounts for regional and local spatial heterogeneity
254 that is not explained by climate, and sampling over source population variance accounts for
255 genetically-based demographic differences across the species' range.

256 Life Table Response Experiments

257 We conducted two types of Life Table Response Experiments (LTRE) to isolate contributions of
258 climate variables and sex-specific vital rates to variation in λ . First, to identify which aspect of
259 climate is most important for population viability, we used an LTRE based on a nonparametric
260 model for the dependence of λ on parameters associated with seasonal temperature and
261 precipitation (Ellner et al., 2016). To do so, we used the RandomForest package to fit a
262 regression model with four climatic variables (temperature of growing season, precipitation of
263 growing season, temperature of the dormant season and precipitation of the dormant season)
264 as predictors and λ calculated from the two sex model as response (Liaw et al., 2002). The
265 regression model allowed the estimation of the relative importance of each predictor.

266 Second, to understand how climate drivers influence λ via sex-specific demography, we
267 decomposed the effect of each climate variable on population growth rate (λ) into contribution
268 arising from the effect on each female and male vital rate using a “regression design” LTRE
269 (Caswell, 1989, 2000). This LTRE decomposes the sensitivity of λ to climate according to:

$$270 \quad \frac{\partial \lambda}{\partial \text{climate}} \approx \sum_i \frac{\partial \lambda}{\partial \theta_i^F} \frac{\partial \theta_i^F}{\partial \text{climate}} + \frac{\partial \lambda}{\partial \theta_i^M} \frac{\partial \theta_i^M}{\partial \text{climate}} \quad (6)$$

271 where, θ_i^F and θ_i^M represent sex-specific parameters (the regression coefficients of the vital
272 rate functions). Because LTRE contributions are additive, we summed across vital rates to
273 compare the total contributions of female and male parameters.

274 Population viability across the climatic niche and geographic range

275 To understand how climate shapes the niche and geographic range of Texas bluegrass, we
276 estimated the probability of self- sustaining populations ($\Pr(\lambda \geq 1)$) conditional to temperature
277 and precipitation of the dormant and growing seasons. $\Pr(\lambda > 1)$ was calculated for the
278 two-sex model and the female dominant MPMs using the proportion of the 300 posterior
279 samples that lead to a $\lambda \geq 1$ (Diez et al., 2014). Population viability in climate niche space
280 was then represented as a contour plot with values of $\Pr(\lambda > 1)$ at given temperature and
281 precipitation for the growing season, holding dormant season climate constant, and vice versa.

282 $\text{Pr}(\lambda > 1)$ was also mapped onto geographic layers of three US states (Texas, Oklahoma
283 and Kansas) to delineate past, current and future potential geographic distribution of the
284 species. To do so, we estimated $\text{Pr}(\lambda > 1)$ conditional to all climate covariates for each
285 pixel ($\sim 25 \text{ km}^2$) for each time period (past, present, future). Because of the amount of the
286 computation involved, we use 100 posterior samples to estimate $\text{Pr}(\lambda > 1)$ across the study
287 area (Texas, Oklahoma and Kansas).

288 **Results**

289 **Sex specific demographic responses and sex ratio variation across climatic
290 conditions**

291 We found strong demographic responses to climate drivers across our Texas bluegrass com-
292 mon garden sites and years, and evidence for demographic differences between the sexes.
293 Regression coefficients related to sex and/or sex:size interactions were significantly non-zero
294 (95% credible intervals excluding zero) for most vital rates (Fig. S-5), suggesting sexual diver-
295 gence in demography. Females generally had an advantage over males, especially in survival
296 and flowering (Fig. 2). Furthermore, there were significant interactions between sex and one or
297 more climate variables, particularly for growth (Fig. S-5B), indicating sexual niche divergence
298 in response to shared climate drivers. Fig. S-6 and S-7 visualize the magnitude of sexual diver-
299 gence in demography across niche space, revealing that female advantages in flowering and
300 panicle production were greatest at both high and low growing season temperature extremes.

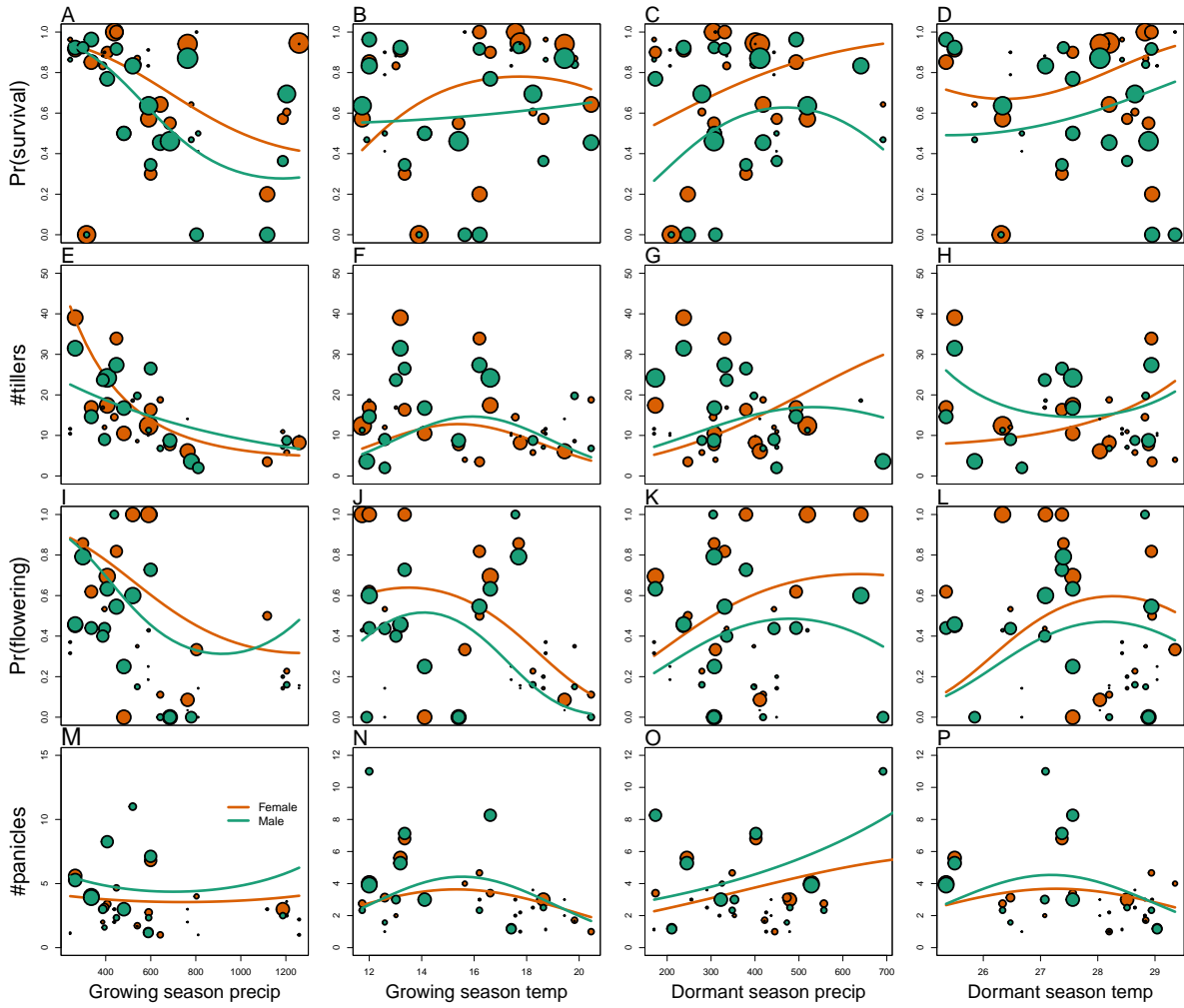


Figure 2: Sex specific demographic response to climate across species range. (A, B, C, D) Probability of survival as a function of precipitation and temperature of the growing and dormant season. (E, F, G, H) Change in number of tillers as a function of precipitation and temperature of the growing and dormant season. (I, J, K, L) Probability of flowering as a function of precipitation and temperature of growing and dormant season. (M, N, O, P) Change in number of panicles as a function of precipitation and temperature of the growing and dormant season. Points show means by site for females (orange) and males (green). Points sizes are proportional to the sample sizes of the mean and are jittered. Lines show fitted statistical models for females (orange) and males (green) based on posterior mean parameter values.

301 Across common garden sites, operational sex ratio (proportion of panicles that are female)
 302 of the experimental populations was female-biased on average ($\approx 60\%$ female), reflecting
 303 the overall greater rates of female vs. male flowering rather than bias in the underlying
 304 population composition. OSR was most female-biased (up to 80% female) at extreme values
 305 of temperature, especially growing season temperature (Fig. S-8, Fig. S-9), consistent with the
 306 female reproductive advantage at temperature extremes seen in the vital rate data (Fig. S-6). In
 307 contrast, there was very little variation in sex ratio (proportion of plants that are female) in the

308 years following common garden establishment (all sites were planted with equal numbers of
309 females and males) and no detectable influence of climate covariates (Fig. S-10), indicating that
310 skew in the OSR comes from sex-biased reproductive rates more so than sex-biased survival.

311 Climate drivers of population viability across niche space

312 Putting all vital rates together in the MPM framework reveals how climate shapes fitness
313 variation across niche dimensions and geographic space, and how accounting for sex structure
314 modifies these inferences. For both female-dominant and two-sex models, fitness variation
315 across niche space was dominated by temperature, with weaker effects of precipitation
316 (compare vertical and horizontal contours in Fig. 3). These visual trends are supported by
317 LTRE decomposition indicating that variation in fitness across climatic conditions is most
318 strongly driven by responses to growing and dormant season temperature, with weaker
319 interactive effects of precipitation that modulate the effects of temperature (Fig. S-12). LTRE
320 analysis also showed that declines in population viability at high and low temperatures were
321 driven most strongly by reductions in vegetative growth and panicle production, with stronger
322 contributions from females than males (Fig. S-13). Intermediate temperatures of both growing
323 and dormant seasons were associated with near-certain projections of population viability
324 ($Pr(\lambda \geq 1) \approx 1$), and high and low temperature extremes during both seasons were associated
325 with low niche suitability ($Pr(\lambda \geq 1) < 0.2$). Higher precipitation slightly expanded the range
326 of suitable temperatures during the dormant season (Fig. 3A), and the reverse was true in
327 the growing season (Fig. 3B). Points in Fig. 3 show that climate change forecasted for the
328 common garden locations would move many of them toward lower-suitability regions of niche
329 space associated with high growing and dormant season temperatures (see also Fig. S-14).

330 While the female-dominant and two-sex models were generally in agreement about high
331 confidence in intermediate temperature optima, they differed around the edges of niche space
332 (Fig. 3C,D,S-14). The female-dominant model over-predicted population viability, especially
333 with respect to growing season temperature. For example, the female-dominant model
334 predicted that, for most levels of precipitation, warm growing season (winter) temperatures
335 of $\sim 20^{\circ}\text{C}$ had high suitability ($Pr(\lambda \geq 1) > 0.9$), while the two-sex model indicated that these
336 conditions were most likely unsuitable ($Pr(\lambda \geq 1) < 0.5$). Similarly, at low winter temperatures
337 that the two-sex model identifies with high certainty as unsuitable ($Pr(\lambda \geq 1) < 0.1$), the
338 female-dominant model is more optimistic ($Pr(\lambda \geq 1) > 0.4$). Across growing season climate
339 space, the female-dominant model over-estimates population viability by ca. 9.23%, on
340 average (Fig. 3D, Fig. S-15B). The difference between female-dominant and two-sex models
341 was qualitatively similar but weaker in magnitude for niche dimensions of the dormant

³⁴² season (Fig. 3C, Fig. S-15A). Female-dominant and two-sex models diverged most strongly
³⁴³ in regions of niche space that favored strongly female-biased operational sex ratios (Fig. S-16).
³⁴⁴ This suggests mate limitation as the biological mechanism underlying model differences.
³⁴⁵ The two-sex model accounts for feedbacks between OSR and female fertility, with reduced
³⁴⁶ seed viability at OSR exceeding ~ 75% female panicles (Fig. S-17) Lacking this feedback, the
³⁴⁷ female-dominant model over-predicts population viability in regions of niche space where
³⁴⁸ male flowering is not sufficient to maximize seed set.

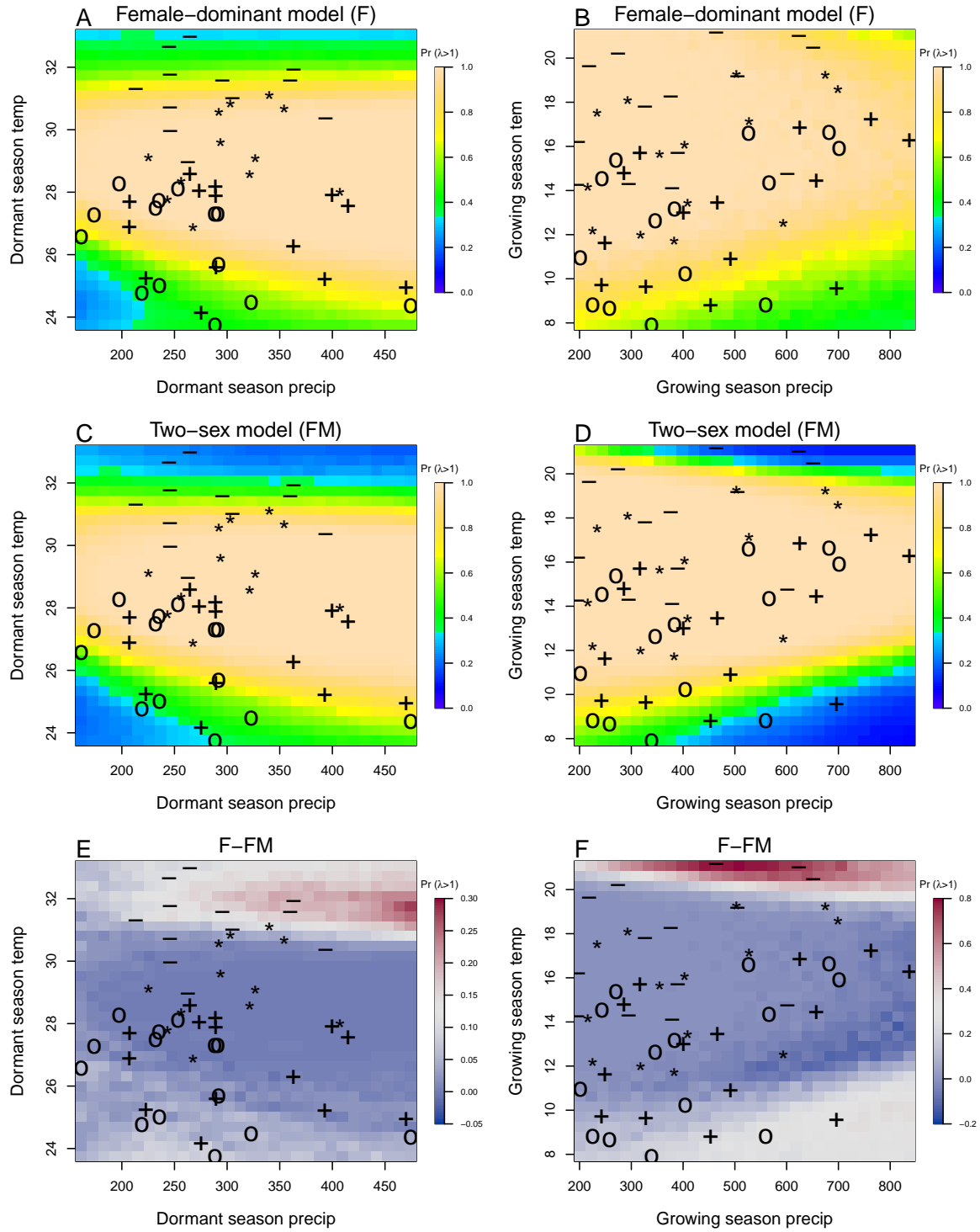


Figure 3: A two-dimensional representation of the predicted niche shift over time (past, present and future climate conditions). "O": Past, "+" Current, "*": RCP 4.5, "-": RCP 8.5.

349 **Climatic change induces shifts in geographic niche and population OSR**

350 Projecting the climatic niche onto geographic space, we find that suitable niche conditions for
351 Texas bluegrass are shifting north under climate change (Fig. 4). Under past (1901-1930) and
352 present (1990-2019) conditions, the two-sex and female-dominant models predict widespread
353 suitability with high confidence ($Pr(\lambda \geq 1) \approx 1$) across much of Texas and Oklahoma. For
354 both models, the predicted geographic niche generally corresponds well to independent ob-
355 servations of the Texas bluegrass distribution (Fig. 4). The predicted geographic niche is more
356 expansive than the GBIF occurrences, particularly at southern, western, and eastern edges, sug-
357 gesting some degree of range disequilibrium (e.g., due to dispersal limitation), geographic bias
358 in occurrence records, and/or model mis-specification. Comparing past to present conditions,
359 the geographic niche for both models has shifted slightly poleward, with reductions in viability
360 at the southern margins and expansions of viability at northern margins. The northward shift
361 of suitable niche conditions is even more pronounced in projections to end-of-century (2071-
362 2100) conditions, with the most dramatic changes in the most pessimistic (RCP8.5) scenario
363 (Fig. 4). In fact, under the pessimistic scenario, Texas bluegrass will have very little remaining
364 climate suitability in the state of Texas by the end of the 21st century. The predicted poleward
365 niche shift is consistent across different global circulation models (Fig. S-22, Fig. S-23, Fig. S-24).

366 Female-dominant and two-sex models are in broad agreement about northward
367 migration of the climatic niche, but the geographic projections reveal hotspots of disagreement
368 where the female-dominant model over-predicts climate suitability and under-predicts the
369 likelihood of range shifts (Fig. 4). These hotspots are generally regions of predicted female
370 bias in the operational sex ratio (Fig. S-18). The strongest contrast between the two models
371 is in the pessimistic climate change scenario (RCP8.5), where the female-dominant model
372 over-predicts population viability by as much as 20% across much of the region (Fig. S-25) and
373 thus under-estimates the magnitude of a potential range shift. In this scenario, a broad swath
374 of the current distribution that is forecasted to be effectively unsuitable ($Pr(\lambda \geq 1) \approx 0$) by the
375 two-sex model is identified as marginally suitable ($Pr(\lambda \geq 1) \approx 0.5$) by the female-dominant
376 model. Accordingly, the OSR of Texas bluegrass across its range is projected to be ca. 75%
377 female panicles, on average, by end of century under RCP8.5, an increase from ca. 60% female
378 under projections for past and current conditions (Fig. 5). The more optimistic climate change
379 scenario (RCP4.5) predicts an intermediate shift in OSR, with hotspots of change at northern
380 and southern range edges becoming strongly female-biased but most of the range remaining
381 near current levels of 60% female (Fig. 5; Fig. S-21, Fig. S-19, Fig. S-20).

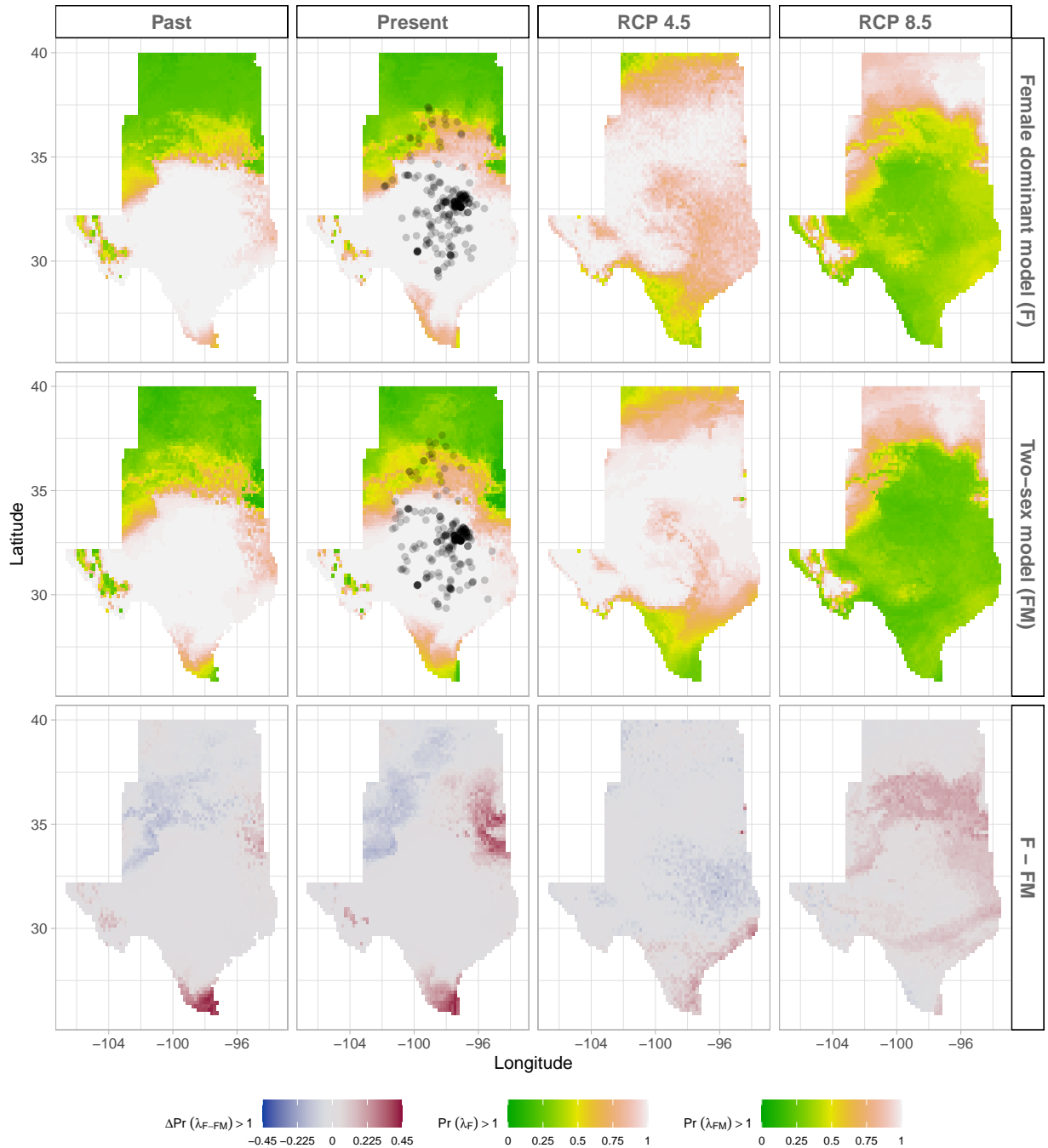


Figure 4: Climate change favors range shift towards north edge. (A) Past, (B) Current, (C and D) Future predicted range shift based on the predicted probabilities of self- sustaining populations, $\text{Pr}(\lambda > 1)$, using the two-sex model that incorporates sex- specific demographic responses to climate with sex ratio dependent seed fertilization. (E) Past, (F) Current, (G and H) Future predicted range shift based on the predicted probabilities of self- sustaining populations, $\text{Pr}(\lambda > 1)$, using the female dominant model. Future projections were based on the CMCC-CM model. The black dots on panel B and F indicate all known presence points collected from GBIF. The occurrences of GBIFs are distributed in with higher population fitness habitat $\text{Pr}(\lambda > 1)$, confirming that our study approach can reasonably predict range shifts.

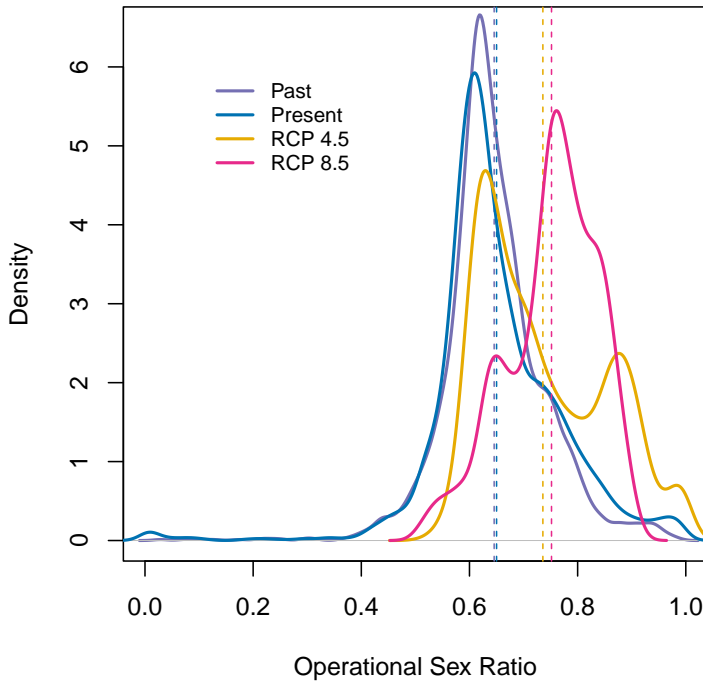


Figure 5: Change in Operational Sex Ratio (proportion of female panicle) over time (past, present, future). Future projections were based on the CMCC-CM model. The mean sex ratio for each time period is shown as vertical dashed line.

382 Discussion

383 Dioecious species make up a large fraction of Earth's biodiversity – most animals and many
 384 plants – yet we have little knowledge about how sex-specific demography and responses to
 385 climate drivers may affect population viability and range shifts of dioecious species under
 386 climate change. We used demographic data collected from common garden experiments,
 387 hierarchical Bayesian statistical modeling, and sex-structured demographic modeling to
 388 forecast for the first time the likely impact of climate change on range dynamics of a dioecious
 389 species. We found that demographic rates of Texas bluegrass and their sensitivities to climate
 390 drivers show significant sex bias, with females out-performing males, on average, and high
 391 and low temperature extremes disproportionately favoring female reproduction, leading to
 392 female skew in the operational sex ratio. In fact, we show that future climate change will likely
 393 not only shift this species' geographic niche northward, but it will also skew operational sex
 394 ratios toward stronger female bias. Our two-sex modeling framework accounts for reductions
 395 in female fertility with increasing female bias, and therefore predicts a narrower climatic niche

396 than the corresponding female-dominant model that ignores the feedback between population
397 structure and vital rates. Failure to account for population sex structure can therefore lead to
398 overestimation of suitable niche space and underestimation of range shifts under global change.

399 Our finding that climate change in the south-central US will likely lead to female-biased
400 operational sex ratios contrasts with previous studies of dioecious plants. While a baseline
401 female demographic advantage has been observed in several dioecious species (Bawa, 1980;
402 Sasaki et al., 2019; Zhao et al., 2012), focused on sex-specific sensitivity to climate drivers
403 predict an increase in male frequency in response to climate change (Hultine et al., 2016; Petry
404 et al., 2016). We speculate that differences in the costs of reproduction related to pollination
405 mode may help explain which sex is favored under climate stress. For most dioecious plant
406 species, the cost of reproduction is often higher for females than males due to the requirement
407 to develop seeds and fruits (Hultine et al., 2016). However, several studies reported a higher
408 cost of reproduction for males in wind pollinated species due to the larger amounts of pollen
409 they produce (Bruijning et al., 2017; Bürli et al., 2022; Cipollini and Whigham, 1994; Field
410 et al., 2013). Additional comparative studies across species that differ in life history traits
411 are needed to draw inferences regarding which types of species are likely to become female-
412 or male-biased in response to global change stressors.

413 While a two-sex modeling approach clearly adds biological realism, it was also additional
414 work (in the form of experiments, data, equations, code, and computation). Was it worth the
415 trouble? Generally, we suggest the answer should depend on the aims of the investigator.
416 Predictions of the sex-structured and female-dominant models were in strong agreement about
417 climate niche optima, and LTRE decomposition suggested that female vital rates determine
418 population responses to climate variation much more so than male vital rates. If we wanted
419 to know whether a poleward range shift is likely for Texas bluegrass, the simpler female-
420 dominant approach could have given us the correct answer. But more focused questions,
421 especially around the edges of niche space where sex ratio skew is more likely to impair
422 population viability, may require an explicit accounting for sex structure. If we aimed to
423 identify specific regions that are more or less inclined toward contraction or expansion, or sites
424 that might be suitable for assisted migration, we might reach qualitatively different conclusions
425 with female-dominant and two-sex models. For example, the female-dominant model is over-
426 confident that large swaths of Oklahoma will remain marginally suitable for Texas bluegrass
427 under the business-as-usual emissions scenario, while the two-sex model is more pessimistic,
428 because this region will become too female-biased to support viable populations. More
429 generally, we hypothesize that accounting for sex structure should be most important under
430 conditions that are already near the limits of population viability, where effects of mate
431 limitation could be more consequential. This suggests a particularly important role of sex-

432 structured modeling for threatened and endangered species, as conservation biologists have
433 already recognized (Jenouvrier et al., 2012; Milner-Gulland, 1994; Molnár et al., 2010).

434 Our results suggest that climate change, and specifically climate warming, will
435 drive a classic pattern of poleward expansion: contraction at the southern trailing edge
436 due to temperatures exceeding tolerable limits and expansion at the northern leading
437 edge due to release from low temperature limitation. Our statistical models captured
438 temperature-dependence in a phenomenological way, and the physiological mechanisms
439 underlying these responses remain to be explored. Increasing temperature could increase
440 evaporative demand, affect plant phenology (Iler et al., 2019; McLean et al., 2016; Sherry et al.,
441 2007), and germination rate (Reed et al., 2021). The potential for temperature to influence
442 these different processes changes seasonally (Konapala et al., 2020). For example, studies
443 suggested that species that are active during the growing season such as cool grass species
444 can have delayed phenology in response to global warming, particularly if temperatures rise
445 above their physiological tolerances (Cleland et al., 2007; Williams et al., 2015).

446 Regardless of the mechanism, it is clear that climate warming will generate leading
447 and trailing edges. Whether and at what pace the realized species' distribution tracks
448 geographic changes in suitable niche space is a different, open question. Expansion of the
449 leading edge could lag behind availability of suitable habitat due to dispersal limitation
450 (Pagel et al., 2020), and legacies of long-lived individuals can promote persistence of trailing
451 edge populations even as environmental conditions deteriorate (Margaret EK et al., 2023).
452 Environmentally-explicit demographic models are emerging as powerful tools to understand
453 and predicts the limits of population viability under global change (Merow et al., 2017;
454 Schultz et al., 2022), but incorporating non-equilibrium dynamics that emerge from dispersal
455 limitation and and historical legacies is an important new direction for this field.

456 Our forecasts for responses to climate change in Texas bluegrass should be interpreted
457 in light of several features of our study design. First, the design of our common garden
458 experiment and statistical modeling means that our geographic projections correspond to an
459 "average" genotype from across the range of Texas bluegrass. Local adaptation to climate could
460 make southern and northern edge populations more resilient to high and low temperature
461 stress, respectively, than the range-wide average (Angert et al., 2020; Gilbert et al., 2017). The
462 role of local adaptation in mitigating population response to climate is an important next
463 step in forecasting species' responses to global change . Second, as is true for many ecological
464 systems, future climate is likely to include conditions that have no present-day analog
465 (Intergovernmental Panel On Climate Change (Ipcc), 2023), a major challenge for ecological
466 forecasting. The years and locations of our experiment provided us with unusually good
467 coverage of likely past, present, and future conditions expected throughout the study region,

468 but we still had to extrapolate the statistical models to predict responses to colder winter
469 temperatures (that were more common in the past) and hotter summer temperatures (that
470 are expected in the future) than we directly observed (Fig. 1). By employing a probabilistic
471 measure of niche and geographic suitability ($Pr(\lambda) \geq 1$), our projections account for the
472 uncertainty associated with these extrapolated climate responses, but there would be value
473 in combining the spatiotemporal sampling of a common garden design with experimental
474 manipulations that push systems toward historical and/or future conditions. Third, while
475 we incorporated uncertainty associated with parameter estimation and process error, there
476 is additional uncertainty in future climate conditions. Future forecasts for Texas bluegrass
477 were generally consistent across different global circulation models (reference supp figures),
478 but combining uncertainty in future conditions alongside uncertainty in biological responses
479 to those conditions is an important frontier in ecological forecasting (Dietze et al., 2018).

480 Conclusion

481 We investigated how demographic differences between the sexes and contrasting sensitivity to
482 climate can drive skewness in sex ratio on and possible range shifts in the context of climate
483 change. For Texas bluegrass, the future is female, and it is in Kansas. Our results suggest
484 that tracking only females could lead to an underestimation of the effect of climate change
485 on population dynamics, because it misses the feedback between population structure and
486 female fertility. But in broad strokes, a female-dominant perspective tells much of the story,
487 and that will likely be true for dioecious plants and animals with mating systems in which
488 few males can fertilize many females. Our work also provides a framework for predicting
489 the impact of global change on population dynamics and range shifts using probabilistic
490 measures that can incorporate and pick apart the many types of uncertainty that arise when
491 reconstructing the past or forecasting the future.

492 Acknowledgements

493 This research was supported by National Science Foundation Division of Environmental
494 Biology awards 2208857 and 2225027. We thank the organizations and institutions who hosted
495 us at their field station facilities, including The Nature Conservancy, Sam Houston State
496 University, University of Texas, Texas A&M University, Texas Tech University, Lake Lewisville
497 Environmental Learning Area, Wichita State University, and Pittsburgh State University.

498 **References**

- 499 Angert, A. L., Bontrager, M. G., and Ågren, J. (2020). What do we really know about adaptation
500 at range edges? *Annual Review of Ecology, Evolution, and Systematics*, 51(1):341–361.
- 501 Bawa, K. S. (1980). Evolution of dioecy in flowering plants. *Annual review of ecology and
502 systematics*, 11:15–39.
- 503 Bertrand, R., Lenoir, J., Piedallu, C., Riofrío-Dillon, G., De Ruffray, P., Vidal, C., Pierrat, J.-C.,
504 and Gégout, J.-C. (2011). Changes in plant community composition lag behind climate
505 warming in lowland forests. *Nature*, 479(7374):517–520.
- 506 Bruijning, M., Visser, M. D., Muller-Landau, H. C., Wright, S. J., Comita, L. S., Hubbell, S. P.,
507 de Kroon, H., and Jongejans, E. (2017). Surviving in a cosexual world: A cost-benefit
508 analysis of dioecy in tropical trees. *The American Naturalist*, 189(3):297–314.
- 509 Bürli, S., Pannell, J. R., and Tonnabel, J. (2022). Environmental variation in sex ratios and
510 sexual dimorphism in three wind-pollinated dioecious plant species. *Oikos*, 2022(6):e08651.
- 511 Caswell, H. (1989). Analysis of life table response experiments i. decomposition of effects
512 on population growth rate. *Ecological Modelling*, 46(3-4):221–237.
- 513 Caswell, H. (2000). *Matrix population models*, volume 1. Sinauer Sunderland, MA.
- 514 Cipollini, M. L. and Whigham, D. F. (1994). Sexual dimorphism and cost of reproduction
515 in the dioecious shrub *lindera benzoin* (lauraceae). *American Journal of Botany*, 81(1):65–75.
- 516 Cleland, E. E., Chuine, I., Menzel, A., Mooney, H. A., and Schwartz, M. D. (2007). Shifting
517 plant phenology in response to global change. *Trends in ecology & evolution*, 22(7):357–365.
- 518 Compagnoni, A., Steigman, K., and Miller, T. E. (2017). Can't live with them, can't live
519 without them? balancing mating and competition in two-sex populations. *Proceedings of
520 the Royal Society B: Biological Sciences*, 284(1865):20171999.
- 521 Czachura, K. and Miller, T. E. (2020). Demographic back-casting reveals that subtle
522 dimensions of climate change have strong effects on population viability. *Journal of Ecology*,
523 108(6):2557–2570.
- 524 Dahlgren, J. P., Bengtsson, K., and Ehrlén, J. (2016). The demography of climate-driven and
525 density-regulated population dynamics in a perennial plant. *Ecology*, 97(4):899–907.

- 526 Davis, M. B. and Shaw, R. G. (2001). Range shifts and adaptive responses to quaternary
527 climate change. *Science*, 292(5517):673–679.
- 528 Dietze, M. C., Fox, A., Beck-Johnson, L. M., Betancourt, J. L., Hooten, M. B., Jarnevich, C. S.,
529 Keitt, T. H., Kenney, M. A., Laney, C. M., Larsen, L. G., et al. (2018). Iterative near-term
530 ecological forecasting: Needs, opportunities, and challenges. *Proceedings of the National
531 Academy of Sciences*, 115(7):1424–1432.
- 532 Diez, J. M., Giladi, I., Warren, R., and Pulliam, H. R. (2014). Probabilistic and spatially variable
533 niches inferred from demography. *Journal of ecology*, 102(2):544–554.
- 534 Eberhart-Phillips, L. J., Küpper, C., Miller, T. E., Cruz-López, M., Maher, K. H., Dos Remedios,
535 N., Stoffel, M. A., Hoffman, J. I., Krüger, O., and Székely, T. (2017). Sex-specific early
536 survival drives adult sex ratio bias in snowy plovers and impacts mating system and
537 population growth. *Proceedings of the National Academy of Sciences*, 114(27):E5474–E5481.
- 538 Ehrlén, J. and Morris, W. F. (2015). Predicting changes in the distribution and abundance
539 of species under environmental change. *Ecology letters*, 18(3):303–314.
- 540 Elderd, B. D. and Miller, T. E. (2016). Quantifying demographic uncertainty: Bayesian methods
541 for integral projection models. *Ecological Monographs*, 86(1):125–144.
- 542 Ellis, R. P., Davison, W., Queirós, A. M., Kroeker, K. J., Calosi, P., Dupont, S., Spicer, J. I.,
543 Wilson, R. W., Widdicombe, S., and Urbina, M. A. (2017). Does sex really matter? explaining
544 intraspecies variation in ocean acidification responses. *Biology letters*, 13(2):20160761.
- 545 Ellner, S. P., Adler, P. B., Childs, D. Z., Hooker, G., Miller, T. E., and Rees, M. (2022). A critical
546 comparison of integral projection and matrix projection models for demographic analysis:
547 Comment. *Ecology*.
- 548 Ellner, S. P., Childs, D. Z., Rees, M., et al. (2016). Data-driven modelling of structured
549 populations. *A practical guide to the Integral Projection Model*. Cham: Springer.
- 550 Evans, M. E., Merow, C., Record, S., McMahon, S. M., and Enquist, B. J. (2016). Towards
551 process-based range modeling of many species. *Trends in Ecology & Evolution*, 31(11):860–871.
- 552 Field, D. L., Pickup, M., and Barrett, S. C. (2013). Comparative analyses of sex-ratio variation
553 in dioecious flowering plants. *Evolution*, 67(3):661–672.
- 554 Gamelon, M., Grøtan, V., Nilsson, A. L., Engen, S., Hurrell, J. W., Jerstad, K., Phillips, A. S.,
555 Røstad, O. W., Slagsvold, T., Walseng, B., et al. (2017). Interactions between demography

- 556 and environmental effects are important determinants of population dynamics. *Science*
557 *Advances*, 3(2):e1602298.
- 558 Gerber, L. R. and White, E. R. (2014). Two-sex matrix models in assessing population viability:
559 when do male dynamics matter? *Journal of Applied Ecology*, 51(1):270–278.
- 560 Gilbert, K. J., Sharp, N. P., Angert, A. L., Conte, G. L., Draghi, J. A., Guillaume, F., Hargreaves,
561 A. L., Matthey-Doret, R., and Whitlock, M. C. (2017). Local adaptation interacts with
562 expansion load during range expansion: maladaptation reduces expansion load. *The
563 American Naturalist*, 189(4):368–380.
- 564 Gissi, E., Bowyer, R. T., and Bleich, V. C. (2024). Sex-based differences affect conservation.
565 *Science*, 384(6702):1309–1310.
- 566 Gissi, E., Schiebinger, L., Hadly, E. A., Crowder, L. B., Santoleri, R., and Micheli, F. (2023).
567 Exploring climate-induced sex-based differences in aquatic and terrestrial ecosystems to
568 mitigate biodiversity loss. *nature communications*, 14(1):4787.
- 569 Hernández, C. M., Ellner, S. P., Adler, P. B., Hooker, G., and Snyder, R. E. (2023). An exact
570 version of life table response experiment analysis, and the r package exactltre. *Methods
571 in Ecology and Evolution*, 14(3):939–951.
- 572 Hitchcock, A. S. (1971). *Manual of the grasses of the United States*, volume 2. Courier Corporation.
- 573 Hultine, K. R., Grady, K. C., Wood, T. E., Shuster, S. M., Stella, J. C., and Whitham, T. G. (2016).
574 Climate change perils for dioecious plant species. *Nature Plants*, 2(8):1–8.
- 575 Iler, A. M., Compagnoni, A., Inouye, D. W., Williams, J. L., CaraDonna, P. J., Anderson, A., and
576 Miller, T. E. (2019). Reproductive losses due to climate change-induced earlier flowering are
577 not the primary threat to plant population viability in a perennial herb. *Journal of Ecology*,
578 107(4):1931–1943.
- 579 Intergovernmental Panel On Climate Change (Ipcc) (2023). *Climate Change 2022 – Impacts,
580 Adaptation and Vulnerability: Working Group II Contribution to the Sixth Assessment Report of
581 the Intergovernmental Panel on Climate Change*. Cambridge University Press, 1 edition.
- 582 Jenouvrier, S., Holland, M., Stroeve, J., Barbraud, C., Weimerskirch, H., Serreze, M., and
583 Caswell, H. (2012). Effects of climate change on an emperor penguin population: analysis
584 of coupled demographic and climate models. *Global Change Biology*, 18(9):2756–2770.

- 585 Jones, M. H., Macdonald, S. E., and Henry, G. H. (1999). Sex-and habitat-specific responses
586 of a high arctic willow, *salix arctica*, to experimental climate change. *Oikos*, pages 129–138.
- 587 Karger, D. N., Conrad, O., Böhner, J., Kawohl, T., Kreft, H., Soria-Auza, R. W., Zimmermann,
588 N. E., Linder, H. P., and Kessler, M. (2017). Climatologies at high resolution for the earth's
589 land surface areas. *Scientific data*, 4(1):1–20.
- 590 Kindiger, B. (2004). Interspecific hybrids of *poa arachnifera* × *poa secunda*. *Journal of New
591 Seeds*, 6(1):1–26.
- 592 Konapala, G., Mishra, A. K., Wada, Y., and Mann, M. E. (2020). Climate change will affect
593 global water availability through compounding changes in seasonal precipitation and
594 evaporation. *Nature communications*, 11(1):3044.
- 595 Lee-Yaw, J. A., Kharouba, H. M., Bontrager, M., Mahony, C., Csergő, A. M., Noreen, A. M.,
596 Li, Q., Schuster, R., and Angert, A. L. (2016). A synthesis of transplant experiments and
597 ecological niche models suggests that range limits are often niche limits. *Ecology letters*,
598 19(6):710–722.
- 599 Liaw, A., Wiener, M., et al. (2002). Classification and regression by randomforest. *R news*,
600 2(3):18–22.
- 601 Louthan, A. M., Keighron, M., Kiekebusch, E., Cayton, H., Terando, A., and Morris, W. F.
602 (2022). Climate change weakens the impact of disturbance interval on the growth rate of
603 natural populations of venus flytrap. *Ecological Monographs*, 92(4):e1528.
- 604 Lynch, H. J., Rhainds, M., Calabrese, J. M., Cantrell, S., Cosner, C., and Fagan, W. F. (2014).
605 How climate extremes—not means—define a species' geographic range boundary via a
606 demographic tipping point. *Ecological Monographs*, 84(1):131–149.
- 607 Margaret EK, E., Sharmila MN, D., Heilman, K. A., Tipton, J. R., DeRose, R. J., Stefan, K.,
608 Schultz, E. L., and Shaw, J. D. (2023). The trailing edge is everywhere: tree rings reveal
609 the transient risk of extinction hidden inside climate envelope forecasts. Technical report,
610 Los Alamos National Laboratory (LANL), Los Alamos, NM (United States).
- 611 McLean, N., Lawson, C. R., Leech, D. I., and van de Pol, M. (2016). Predicting when climate-
612 driven phenotypic change affects population dynamics. *Ecology Letters*, 19(6):595–608.
- 613 Merow, C., Bois, S. T., Allen, J. M., Xie, Y., and Silander Jr, J. A. (2017). Climate change both
614 facilitates and inhibits invasive plant ranges in new england. *Proceedings of the National
615 Academy of Sciences*, 114(16):E3276–E3284.

- 616 Miller, T. and Compagnoni, A. (2022a). Data from: Two-sex demography, sexual niche
617 differentiation, and the geographic range limits of texas bluegrass (*Poa arachnifera*). *American*
618 *Naturalist*, Dryad Digital Repository,. <https://doi.org/10.5061/dryad.kkwh70s5x>.
- 619 Miller, T. E. and Compagnoni, A. (2022b). Two-sex demography, sexual niche differentiation,
620 and the geographic range limits of texas bluegrass (*poa arachnifera*). *The American*
621 *Naturalist*, 200(1):17–31.
- 622 Miller, T. E., Shaw, A. K., Inouye, B. D., and Neubert, M. G. (2011). Sex-biased dispersal and
623 the speed of two-sex invasions. *The American Naturalist*, 177(5):549–561.
- 624 Milner-Gulland, E. (1994). A population model for the management of the saiga antelope.
625 *Journal of Applied Ecology*, pages 25–39.
- 626 Molnár, P. K., Derocher, A. E., Thiemann, G. W., and Lewis, M. A. (2010). Predicting survival,
627 reproduction and abundance of polar bears under climate change. *Biological Conservation*,
628 143(7):1612–1622.
- 629 Morrison, C. A., Robinson, R. A., Clark, J. A., and Gill, J. A. (2016). Causes and consequences
630 of spatial variation in sex ratios in a declining bird species. *Journal of Animal Ecology*,
631 85(5):1298–1306.
- 632 Pagel, J., Treurnicht, M., Bond, W. J., Kraaij, T., Nottebrock, H., Schutte-Vlok, A., Tonnabel,
633 J., Esler, K. J., and Schurr, F. M. (2020). Mismatches between demographic niches and
634 geographic distributions are strongest in poorly dispersed and highly persistent plant
635 species. *Proceedings of the National Academy of Sciences*, 117(7):3663–3669.
- 636 Pease, C. M., Lande, R., and Bull, J. (1989). A model of population growth, dispersal and
637 evolution in a changing environment. *Ecology*, 70(6):1657–1664.
- 638 Petry, W. K., Soule, J. D., Iler, A. M., Chicas-Mosier, A., Inouye, D. W., Miller, T. E., and
639 Mooney, K. A. (2016). Sex-specific responses to climate change in plants alter population
640 sex ratio and performance. *Science*, 353(6294):69–71.
- 641 Piironen, J. and Vehtari, A. (2017). Comparison of bayesian predictive methods for model
642 selection. *Statistics and Computing*, 27:711–735.
- 643 Pottier, P., Burke, S., Drobniak, S. M., Lagisz, M., and Nakagawa, S. (2021). Sexual (in) equality?
644 a meta-analysis of sex differences in thermal acclimation capacity across ectotherms.
645 *Functional Ecology*, 35(12):2663–2678.

- 646 R Core Team (2023). *R: A Language and Environment for Statistical Computing*. R Foundation
647 for Statistical Computing, Vienna, Austria.
- 648 Reed, P. B., Peterson, M. L., Pfeifer-Meister, L. E., Morris, W. F., Doak, D. F., Roy, B. A., Johnson,
649 B. R., Bailes, G. T., Nelson, A. A., and Bridgman, S. D. (2021). Climate manipulations
650 differentially affect plant population dynamics within versus beyond northern range limits.
651 *Journal of Ecology*, 109(2):664–675.
- 652 Renganayaki, K., Jessup, R., Burson, B., Hussey, M., and Read, J. (2005). Identification of
653 male-specific aflu markers in dioecious texas bluegrass. *Crop science*, 45(6):2529–2539.
- 654 Sanderson, B. M., Knutti, R., and Caldwell, P. (2015). A representative democracy to reduce
655 interdependency in a multimodel ensemble. *Journal of Climate*, 28(13):5171–5194.
- 656 Sasaki, M., Hedberg, S., Richardson, K., and Dam, H. G. (2019). Complex interactions
657 between local adaptation, phenotypic plasticity and sex affect vulnerability to warming
658 in a widespread marine copepod. *Royal Society open science*, 6(3):182115.
- 659 Schultz, E. L., Hülsmann, L., Pillet, M. D., Hartig, F., Breshears, D. D., Record, S., Shaw, J. D.,
660 DeRose, R. J., Zuidema, P. A., and Evans, M. E. (2022). Climate-driven, but dynamic and
661 complex? a reconciliation of competing hypotheses for species' distributions. *Ecology letters*,
662 25(1):38–51.
- 663 Schwalm, C. R., Glendon, S., and Duffy, P. B. (2020). Rcp8. 5 tracks cumulative co2 emissions.
664 *Proceedings of the National Academy of Sciences*, 117(33):19656–19657.
- 665 Schwinning, S., Lortie, C. J., Esque, T. C., and DeFalco, L. A. (2022). What common-garden
666 experiments tell us about climate responses in plants.
- 667 Sexton, J. P., McIntyre, P. J., Angert, A. L., and Rice, K. J. (2009). Evolution and ecology of
668 species range limits. *Annu. Rev. Ecol. Evol. Syst.*, 40:415–436.
- 669 Shelton, A. O. (2010). The ecological and evolutionary drivers of female-biased sex ratios:
670 two-sex models of perennial seagrasses. *The American Naturalist*, 175(3):302–315.
- 671 Sherry, R. A., Zhou, X., Gu, S., Arnone III, J. A., Schimel, D. S., Verburg, P. S., Wallace,
672 L. L., and Luo, Y. (2007). Divergence of reproductive phenology under climate warming.
673 *Proceedings of the National Academy of Sciences*, 104(1):198–202.
- 674 Smith, M. D., Wilkins, K. D., Holdrege, M. C., Wilfahrt, P., Collins, S. L., Knapp, A. K., Sala,
675 O. E., Dukes, J. S., Phillips, R. P., Yahdjian, L., et al. (2024). Extreme drought impacts have

- 676 been underestimated in grasslands and shrublands globally. *Proceedings of the National*
677 *Academy of Sciences*, 121(4):e2309881120.
- 678 Stan Development Team (2023). RStan: the R interface to Stan. R package version 2.21.8.
- 679 Thomson, A. M., Calvin, K. V., Smith, S. J., Kyle, G. P., Volke, A., Patel, P., Delgado-Arias,
680 S., Bond-Lamberty, B., Wise, M. A., Clarke, L. E., et al. (2011). Rcp4. 5: a pathway for
681 stabilization of radiative forcing by 2100. *Climatic change*, 109:77–94.
- 682 Tognetti, R. (2012). Adaptation to climate change of dioecious plants: does gender balance
683 matter? *Tree Physiology*, 32(11):1321–1324.
- 684 Williams, J. L., Jacquemyn, H., Ochocki, B. M., Brys, R., and Miller, T. E. (2015). Life
685 history evolution under climate change and its influence on the population dynamics of
686 a long-lived plant. *Journal of Ecology*, 103(4):798–808.
- 687 Zhao, H., Li, Y., Zhang, X., Korpelainen, H., and Li, C. (2012). Sex-related and stage-dependent
688 source-to-sink transition in populus cathayana grown at elevated co 2 and elevated
689 temperature. *Tree Physiology*, 32(11):1325–1338.

Supporting Information

690 S.1 Supporting Figures

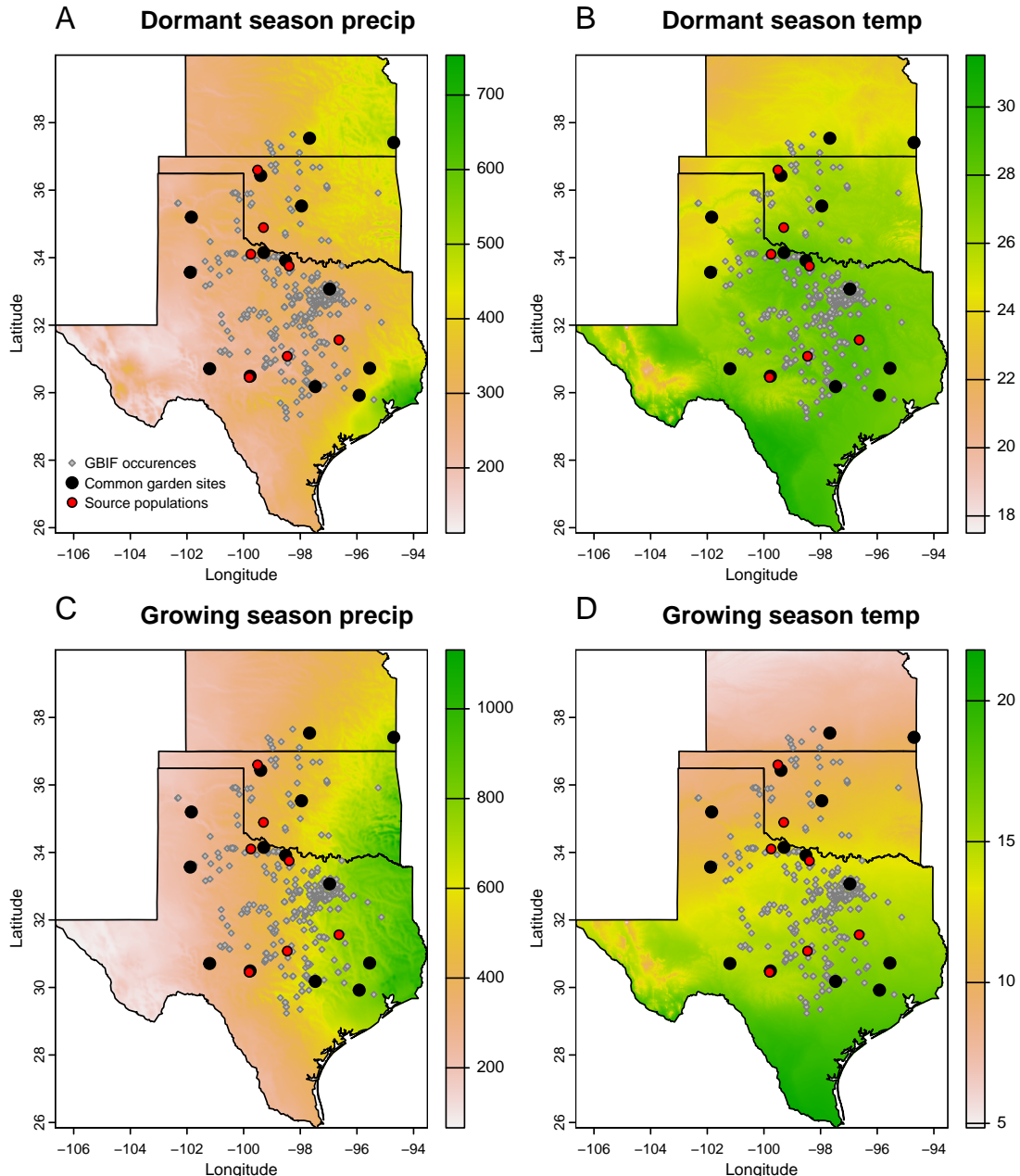


Figure S-1: Maps of 30-year (1990-2019) climate normals and study sites used for demographic monitoring of *Poa arachnifera* in Texas, Kansas and Oklahoma in the United States. Precipitation is in mm and temperature is in °C. We surveyed 22 natural populations (grey diamond). The common garden sites were installed on 14 sites (black circle) collected from 7 sources populations (red circle).

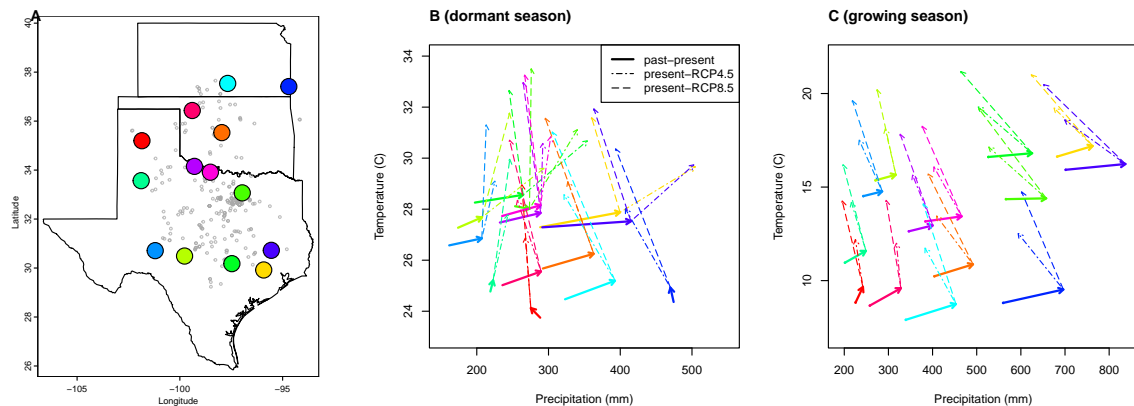


Figure S-2: (A), Common garden locations in Texas, Oklahoma, and Kansas (points) and (B,C) corresponding changes in growing and dormant season climate. Arrows in B,C connect past (1901-1930) and present (1990-2019) climate normals, and present and future (2071-2100) climate normals under RCP4.5 and RCP8.5 forecasts. Future forecasts are from MIROC5 but other climate models show similar patterns.

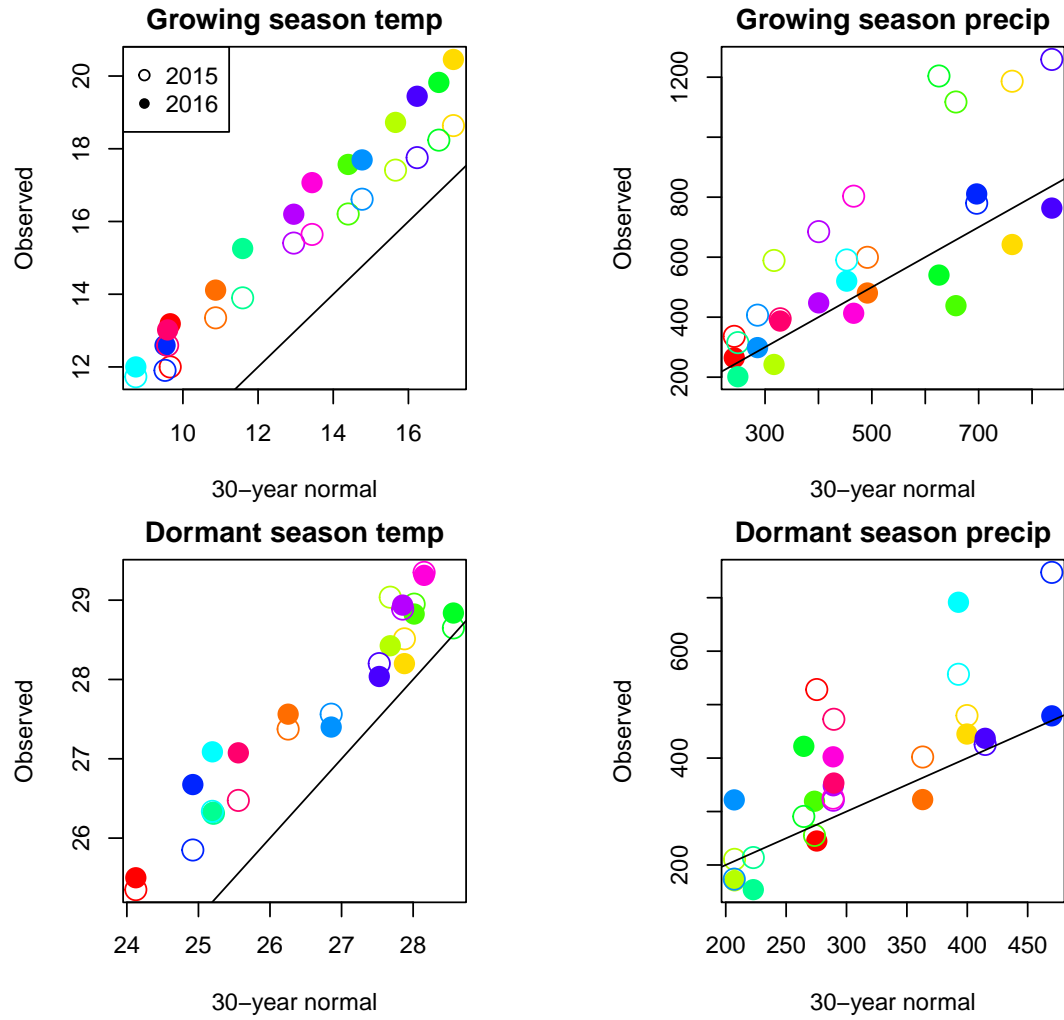


Figure S-3: Comparison of 30-year (1990-2019) climate normals and observed weather conditions at common garden sites during the 2014–15 and 2015–16 census periods. Temperature is in $^{\circ}\text{C}$ and precipitation is in mm . Colors represent sites and lines show the $y=x$ relationship.

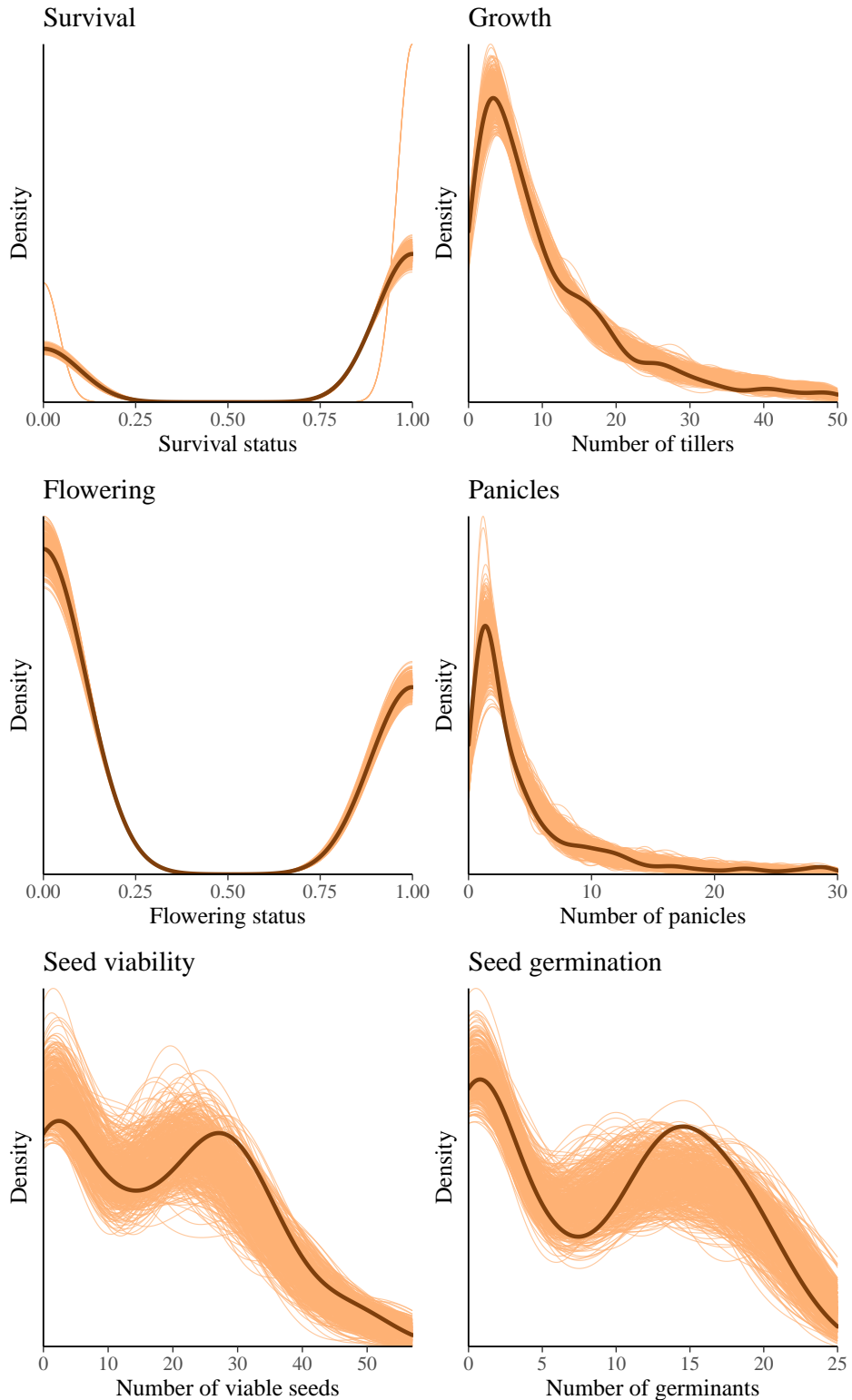


Figure S-4: Posterior predictive checks. Consistency between real data and simulated values suggests that the fitted vital rate models accurately describes the data. Graph shows density curves for the observed data (light orange) along with the simulated values (dark orange).

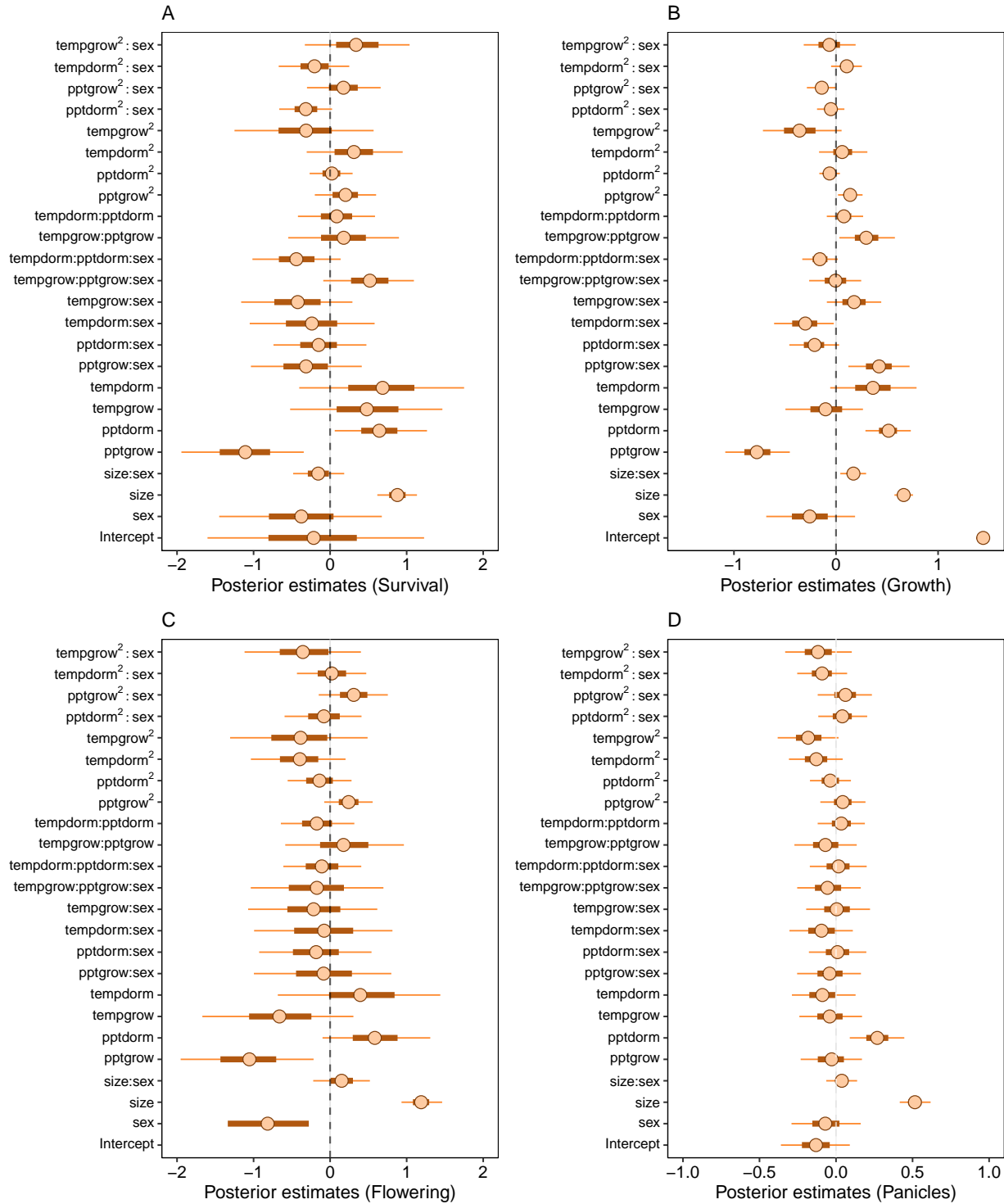


Figure S-5: Mean parameter values and 95% credible intervals of the posterior probability distributions. pptgrow is the precipitation of growing season, Tempgrow is the temperature of growing season, pptdorm is the temperature of dormant season, Tempdorm is the temperature of dormant season.

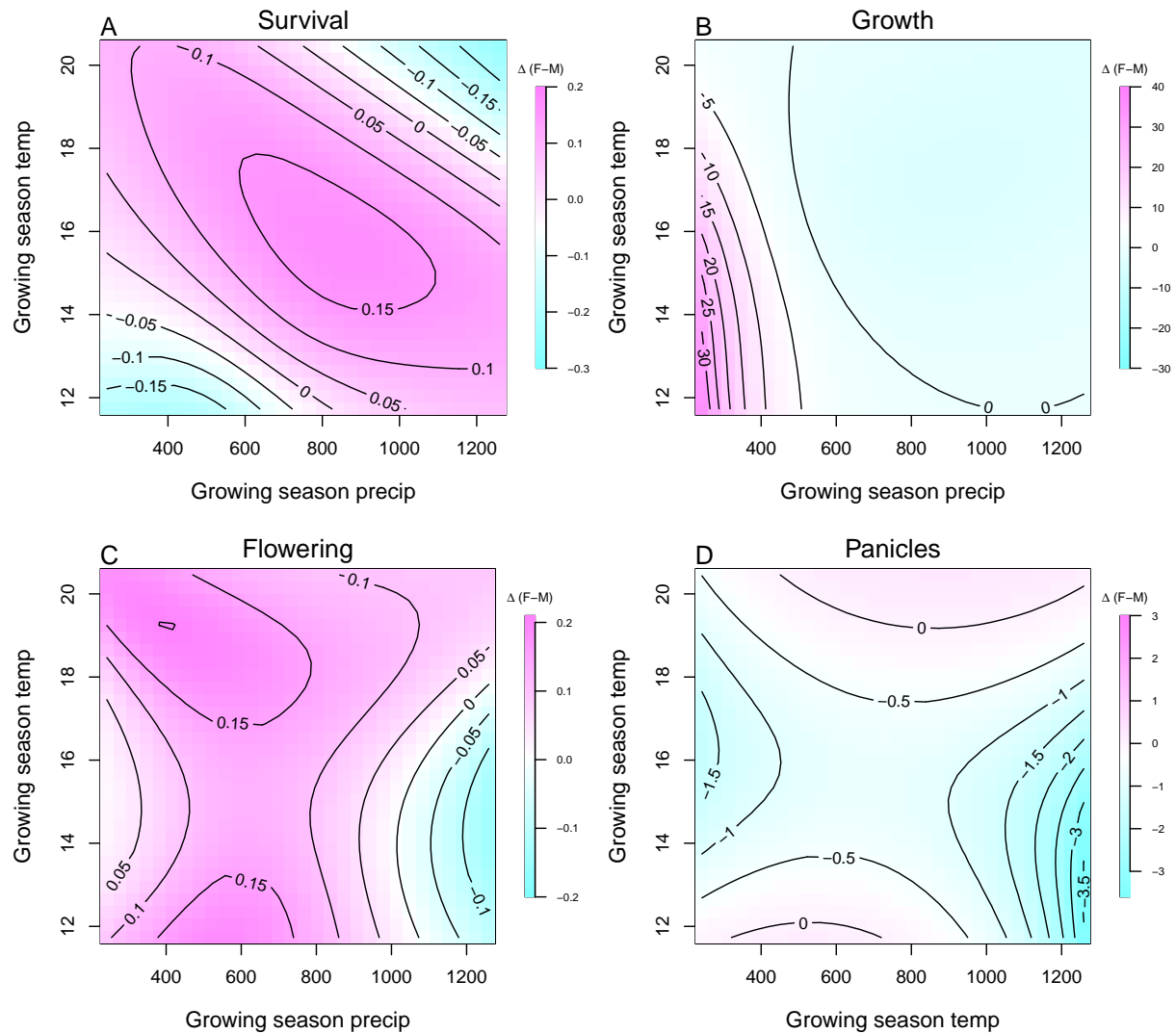


Figure S-6: Predicted difference in demographic response to climate across species range between female and male. Contours show predicted value of that difference conditional on precipitation and temperature of growing season

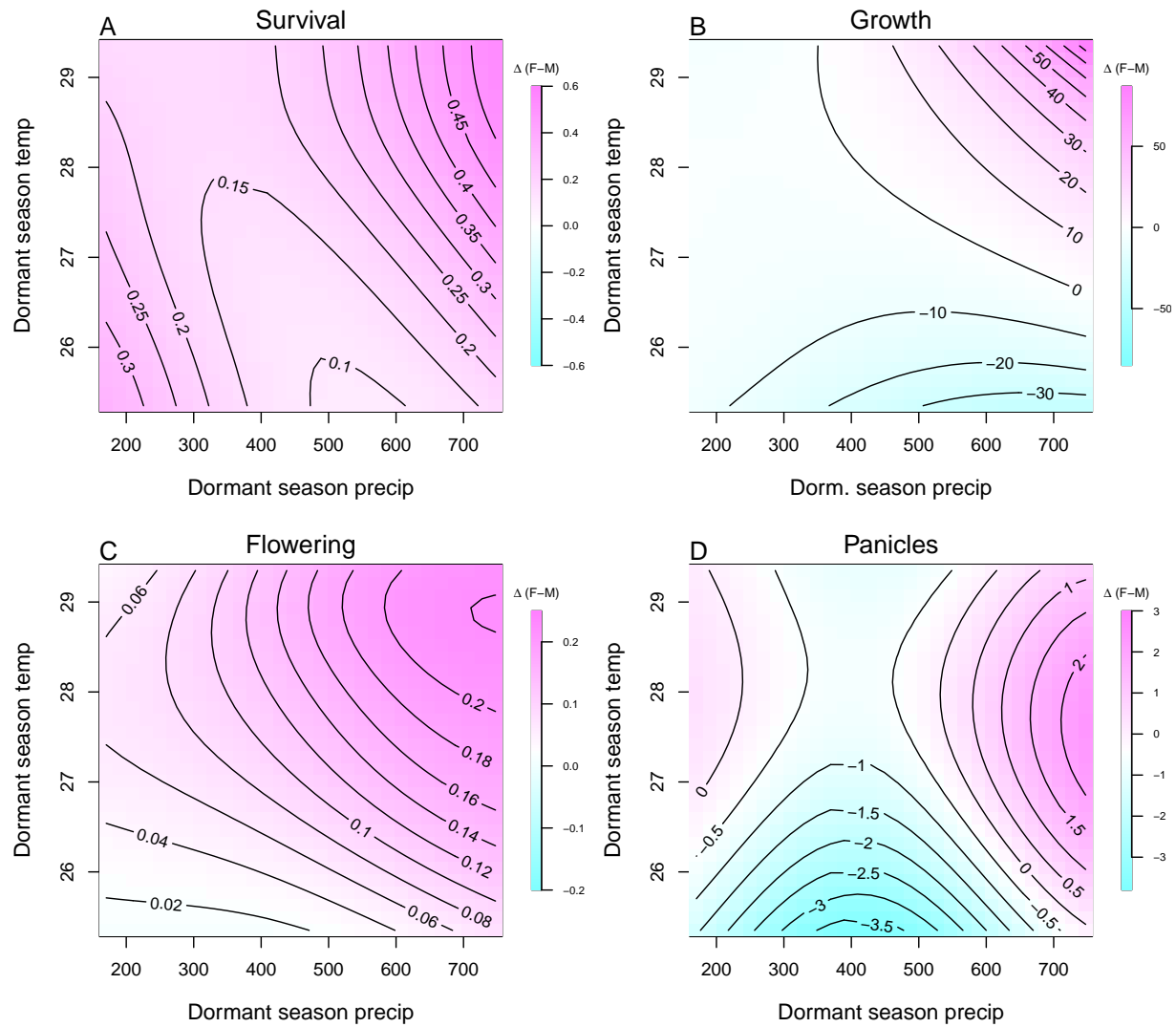


Figure S-7: Predicted difference in demographic response to climate across species range between female and male. Contours show predicted value of that difference conditional on precipitation and temperature of the dormant season

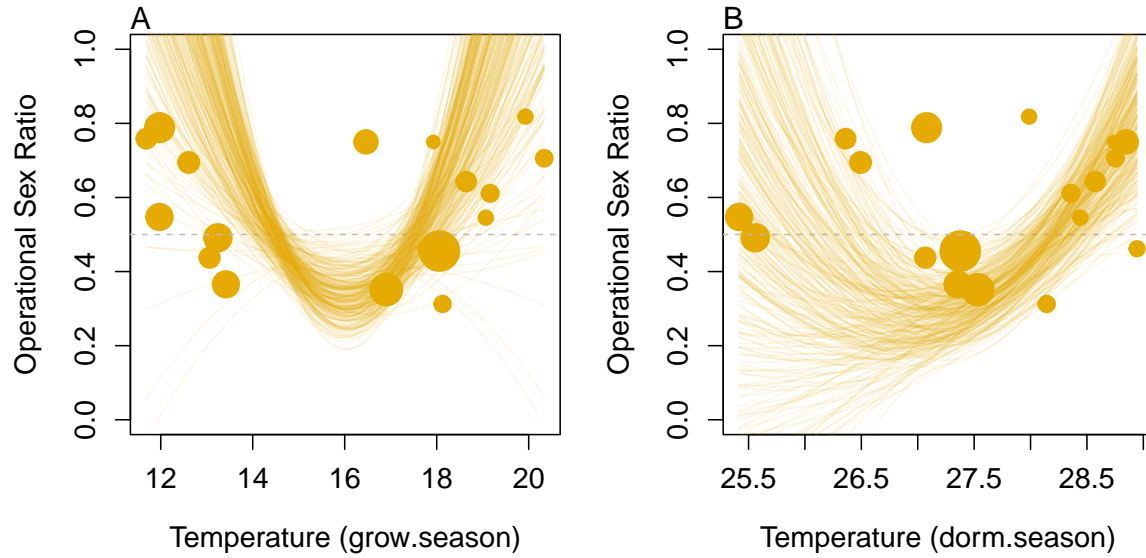


Figure S-8: Significant Operational Sex Ratio response across climate gradient. (A, B) Proportion of panicles that were females across temperature of the growing and dormant season

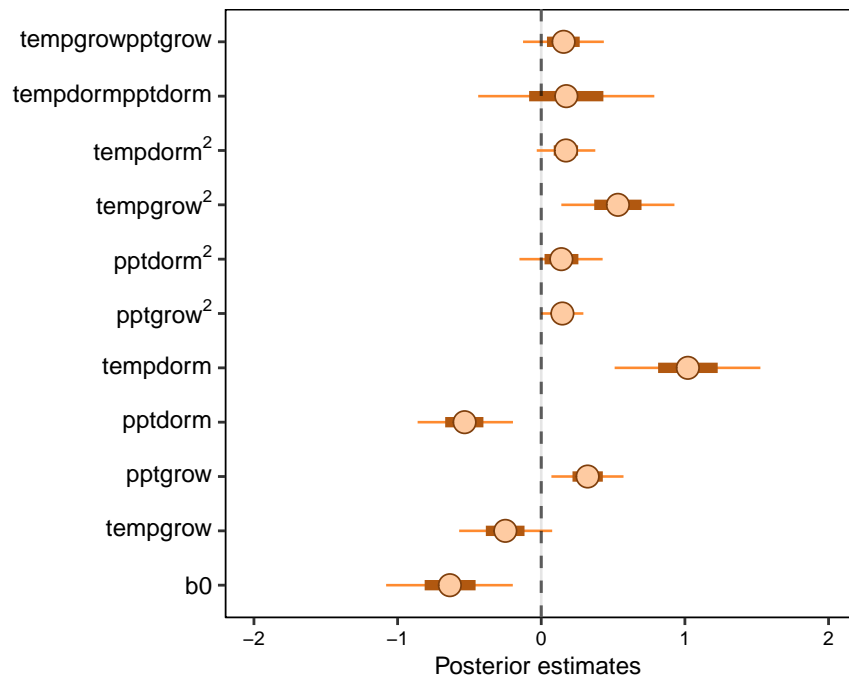


Figure S-9: Mean parameter values and 95% credible intervals of the posterior probability distributions for climate drivers of operational sex ratio (female fraction of total panicles) across common garden years and sites. pptgrow is the precipitation of growing season, Tempgrow is the temperature of growing season, pptdorm is the temperature of dormant season, Tempdorm is the temperature of dormant season.

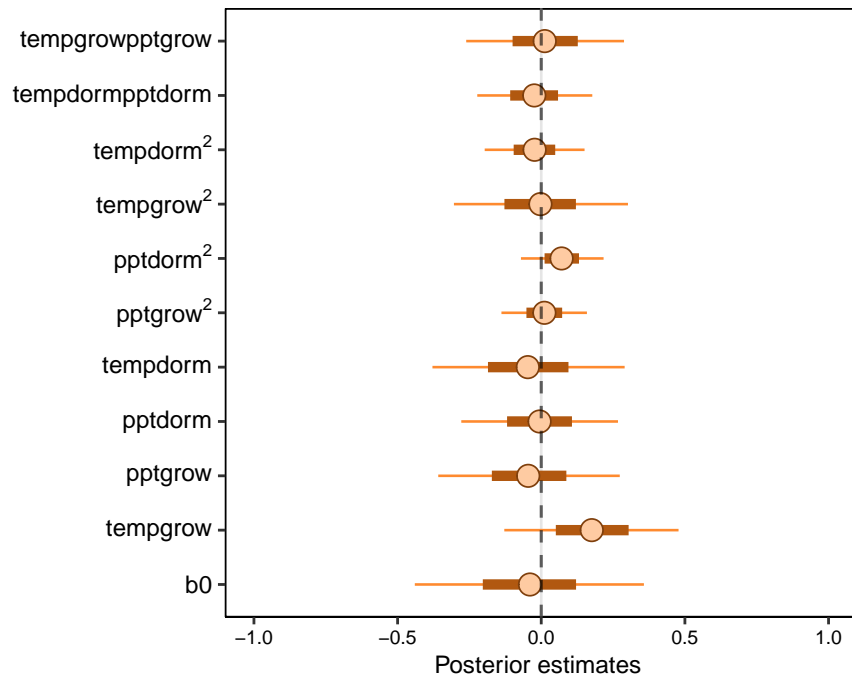


Figure S-10: Mean parameter values and 95% credible intervals of the posterior probability distributions for climate drivers of sex ratio (female fraction of the populations) across common garden years and sites. pptgrow is the precipitation of growing season, Tempgrow is the temperature of growing season, pptdorm is the temperature of dormant season, Tempdorm is the temperature of dormancy.

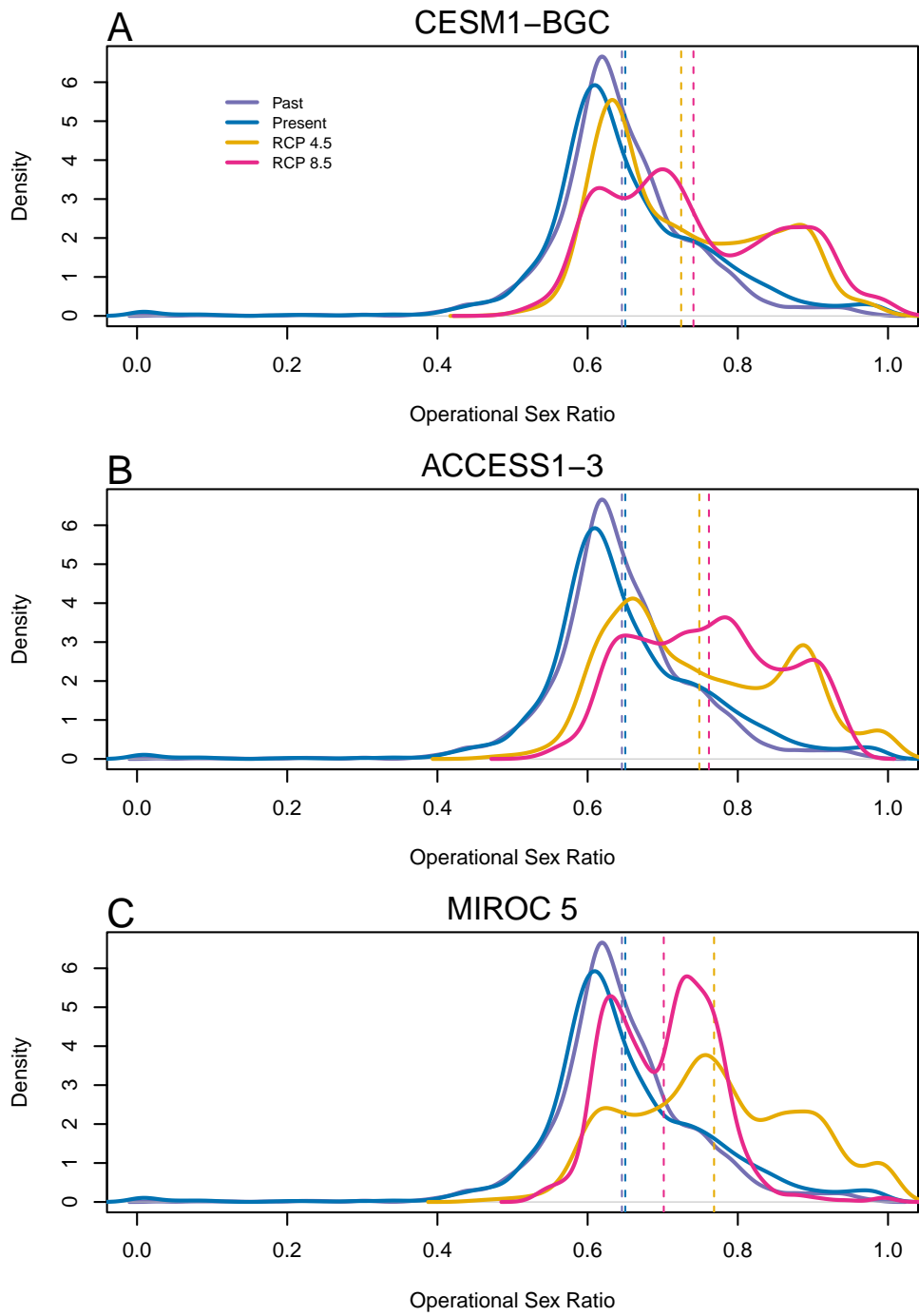


Figure S-11: Change in Operational Sex Ratio (proportion of female) over time (past, present, future). Future projections were based on A) MIROC 5, B) CES, C) ACC. The means for each model are shown as vertical dashed lines.

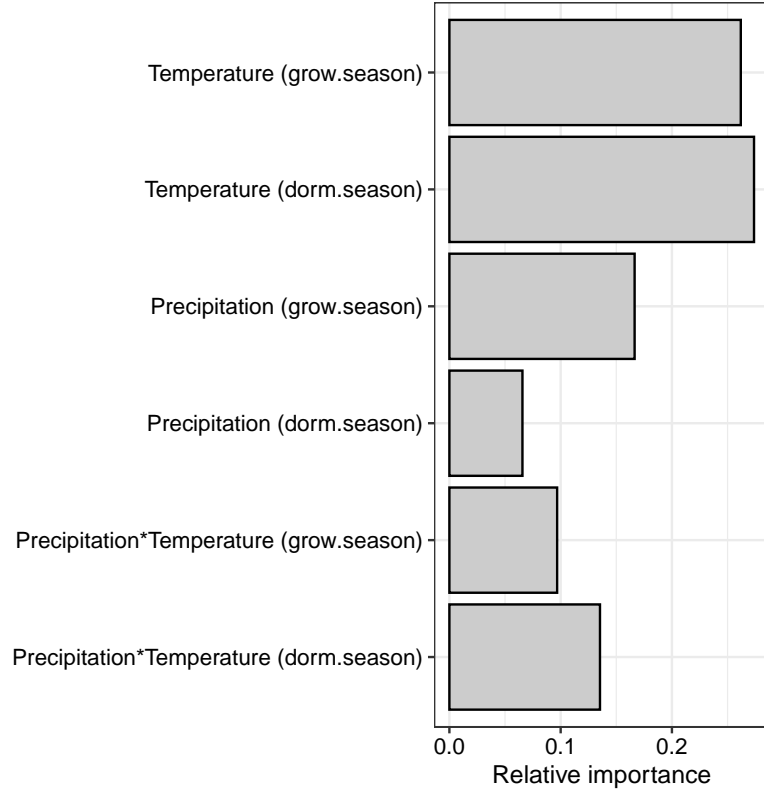


Figure S-12: Life Table Response Experiment: The bar represent the relative importance of each predictors.

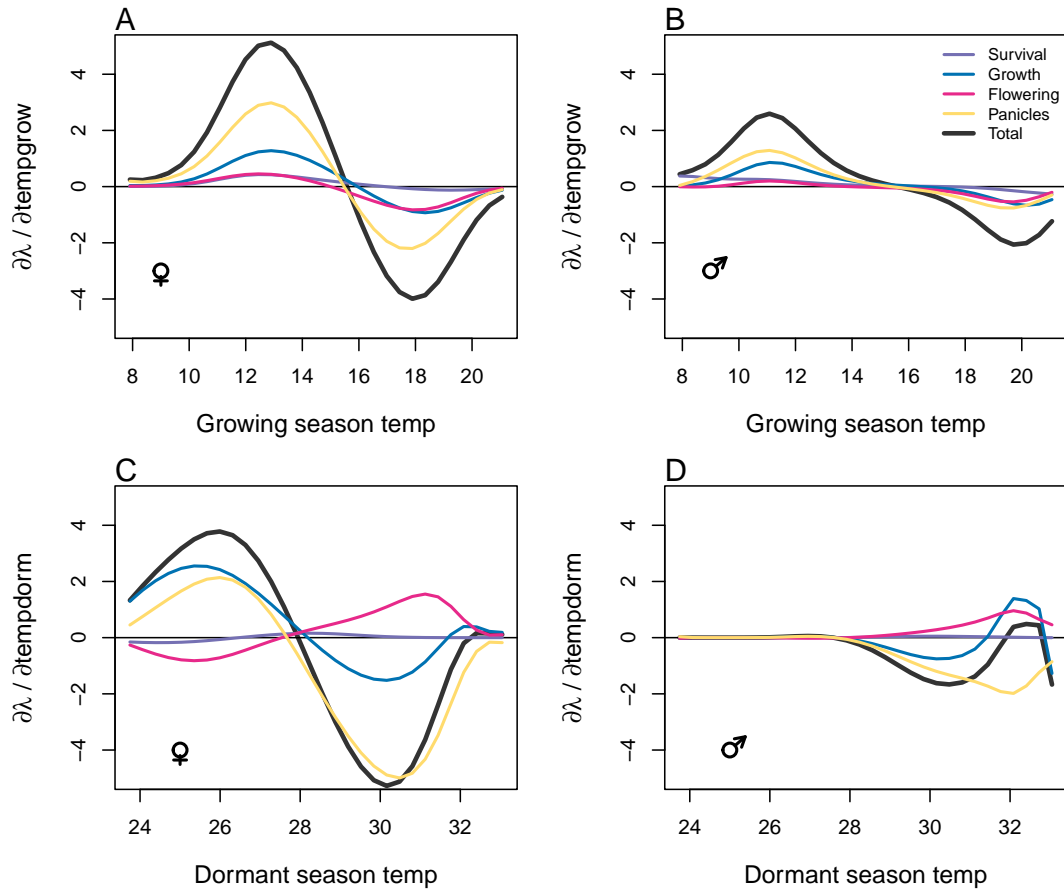


Figure S-13: Life table response experiment decomposition of the sensitivity of λ to seasonal climate into additive vital rate contributions of males and females based on posterior mean parameter estimates. (A) Temperature of growing season (contribution of female), (B) Temperature of growing season (contribution of male), (C) Temperature of dormant season (contribution of female) and (D) Temperature of dormant season (contribution of male).

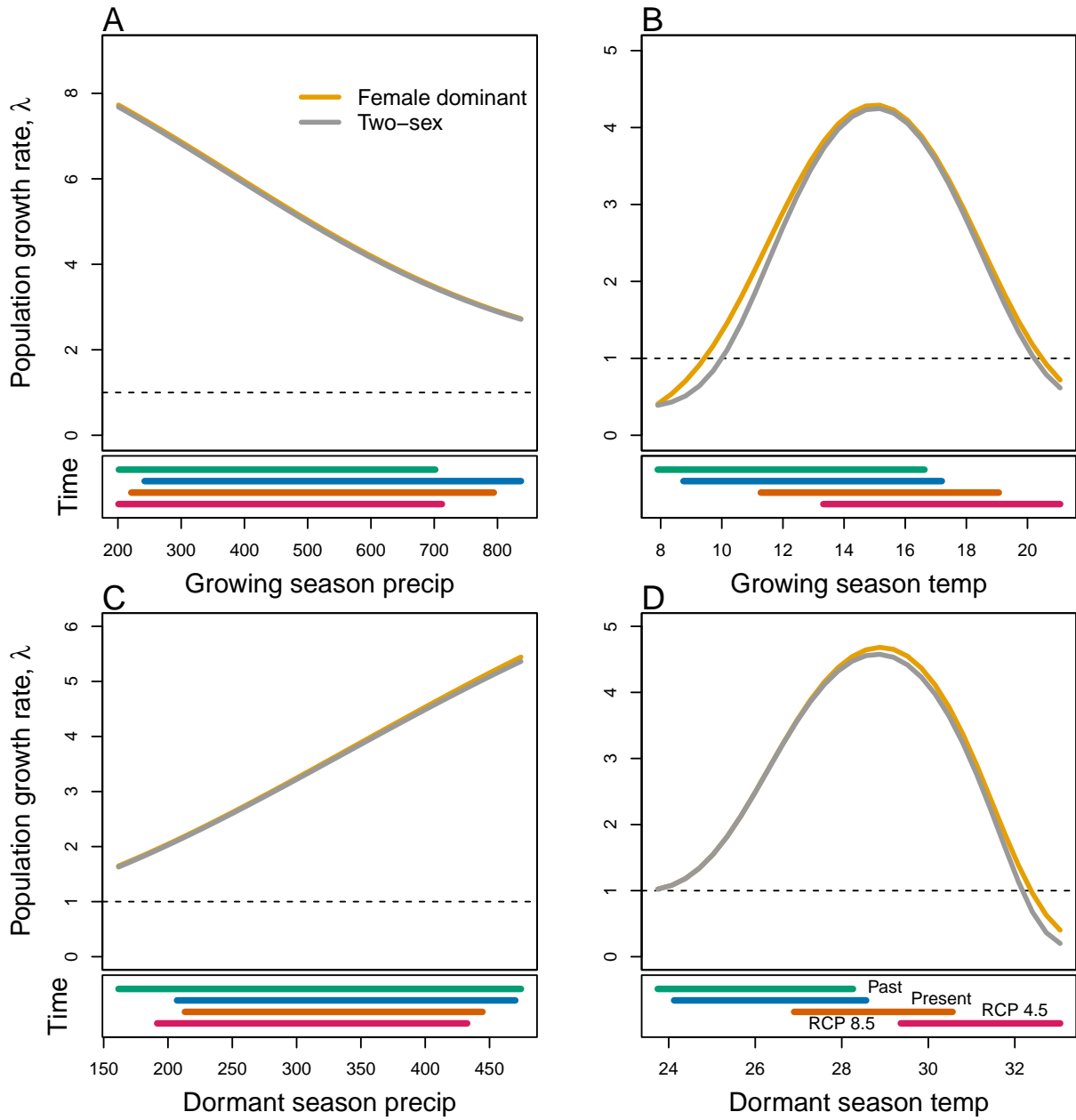


Figure S-14: Predicted population growth rate (λ) in different ranges of climate. (A) Precipitation of the growing season, (B) Temperature of the growing season, (C) Precipitation of the dormant season, (D) Temperature of the dormant season. The grey curve shows prediction by the two-sex matrix projection model that incorporates sex-specific demographic responses to climate with sex ratio dependent seed fertilization. The orange curve represents the prediction by the female dominant matrix projection model. The dashed horizontal line indicates the limit of population viability ($\lambda = 1$). Lower panels below each data panel show ranges of climate values for different time period (past climate, present and future climates). For future climate, we show a Representation Concentration Pathways (RCP) 4.5 and 8.5. Values population viability of (λ) are derived from the mean climate variables across 4 GCMs (MIROC5, ACCESS1-3, CESM1-BGC, CMCC-CM).

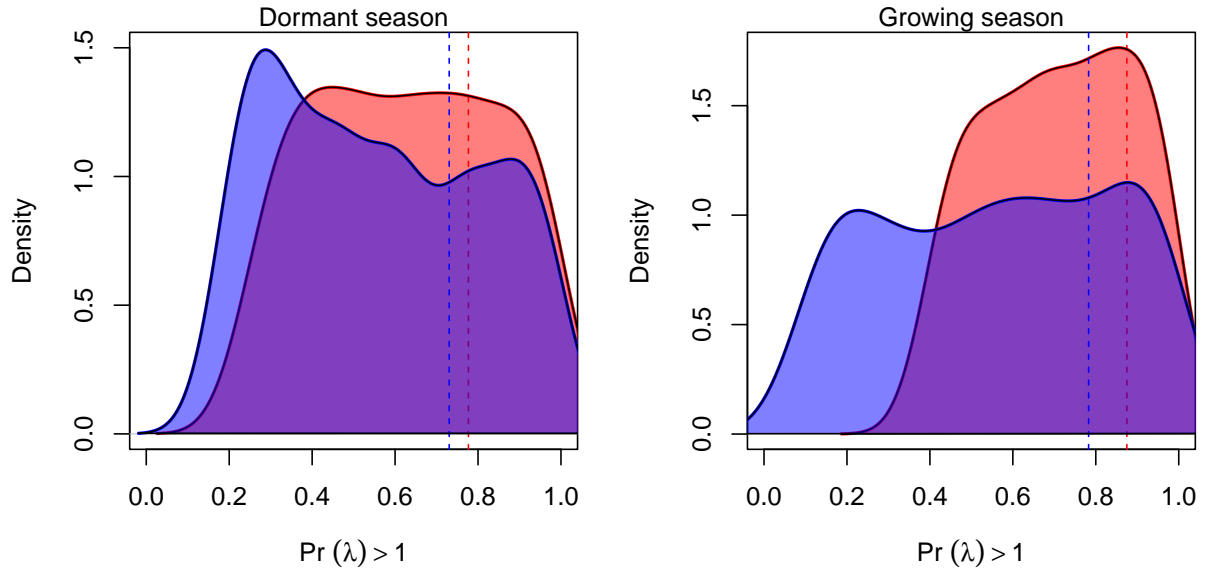


Figure S-15: Assessment of the statistical difference between the two-sex models and the female dominant model for the dormant and growing season. Plots show the density of $\text{Pr}(\lambda > 1)$ values for female dominant (pink) and two-sex models (violet) for each season. The means for each model are shown as vertical dashed lines.

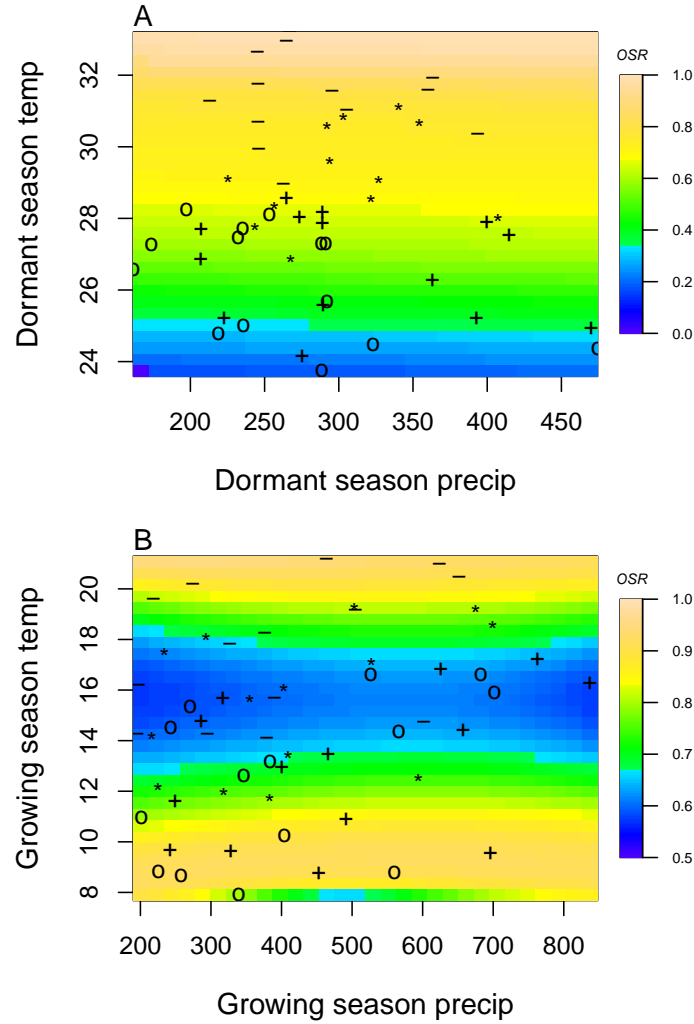


Figure S-16: A two-dimensional representation of the Operational Sex Ratio (OSR) over time (past, present and future climate conditions). OSR represents the proportion of females. Contours show predicted values of OSR conditional on precipitation and temperature of the dormant and growing season. Operational Sex Ratio during the dormant season for the two sex model (A), Operational Sex Ratio during the growing season for the two sex model (B). “**o**”: Past, “**+**”: Current, “*****”: RCP 4.5, “**-**”: RCP 8.5.

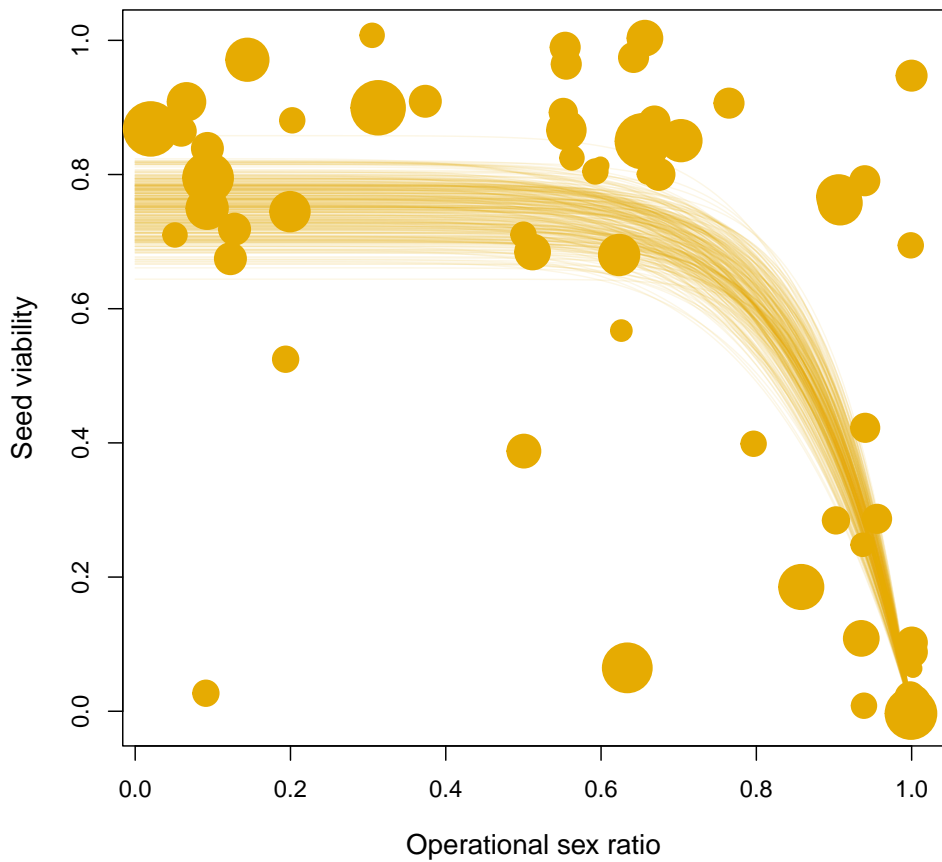


Figure S-17: Seed fertilization success as a function of operational sex ratio (fraction of panicles that are female) in experimental populations. Circles show data from tetrazolium assays of seed viability; circle size is proportional to the number of seeds tested (minimum: 14; maximum: 57). Lines show model predictions for 300 samples from the posterior distribution of parameter estimate

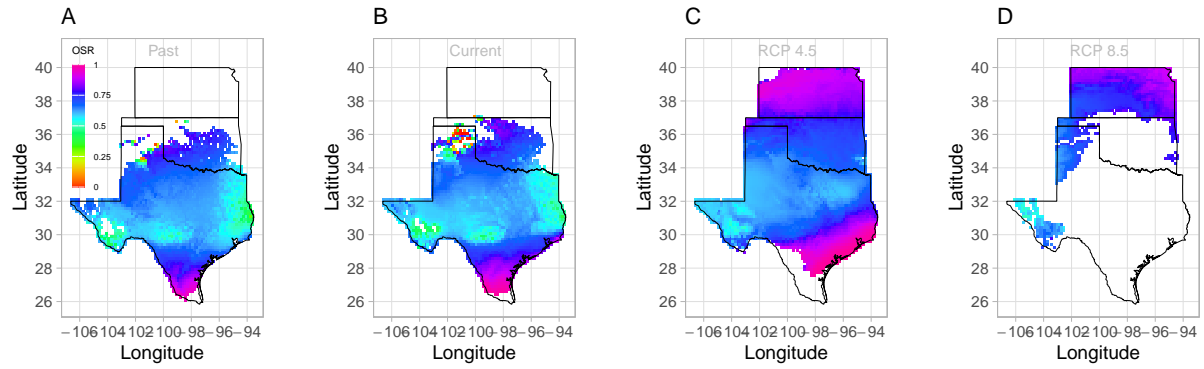


Figure S-18: Projection of Operational Sex Ratio (proportion of female panicle) over time (past, present, future) across species range. Future projections were based on the CMCC-CM model.

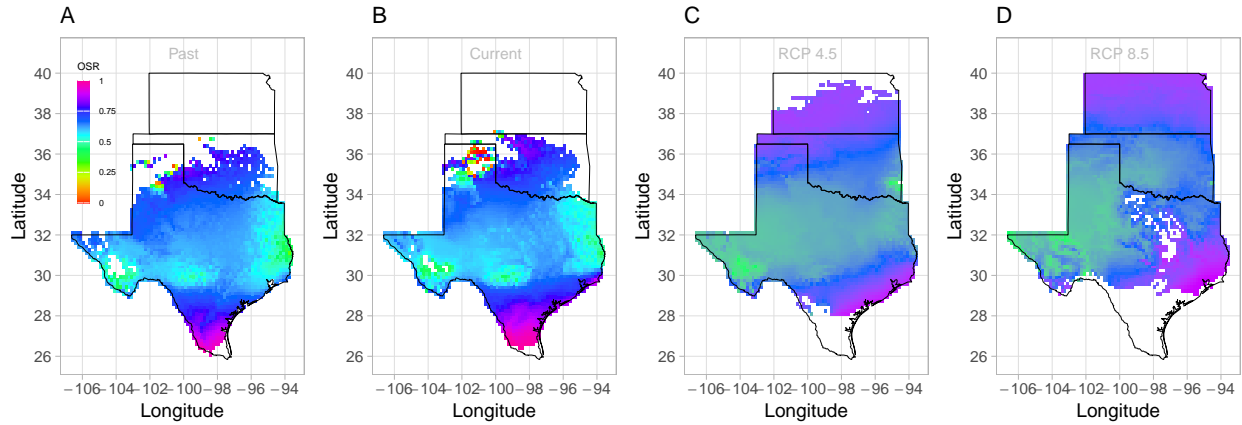


Figure S-19: Projection of in Operational Sex Ratio (proportion of female panicle) over time (past, present, future) across species range. Future projections were based on the CES model.

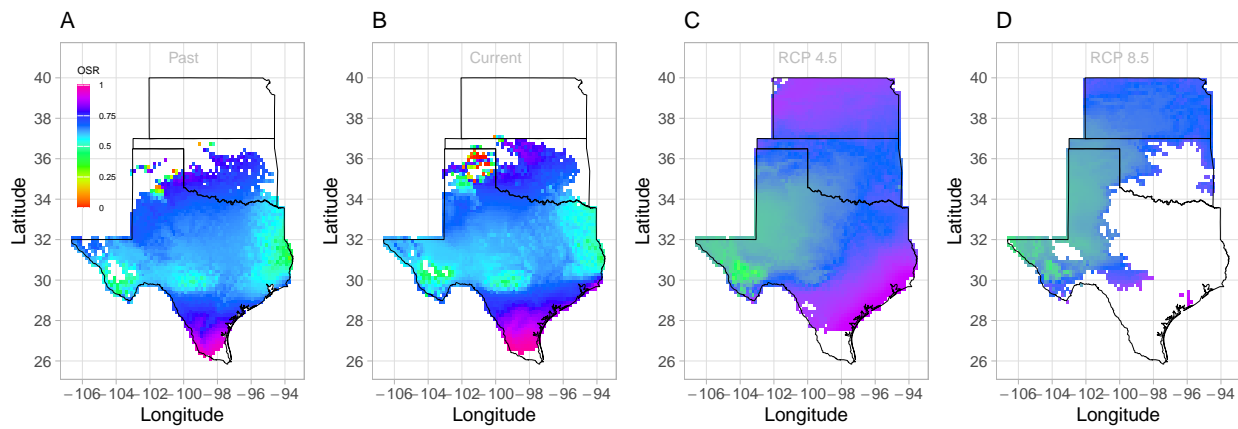


Figure S-20: Projection of Operational Sex Ratio (proportion of female panicle) over time (past, present, future) across species range. Future projections were based on the MIROC model.

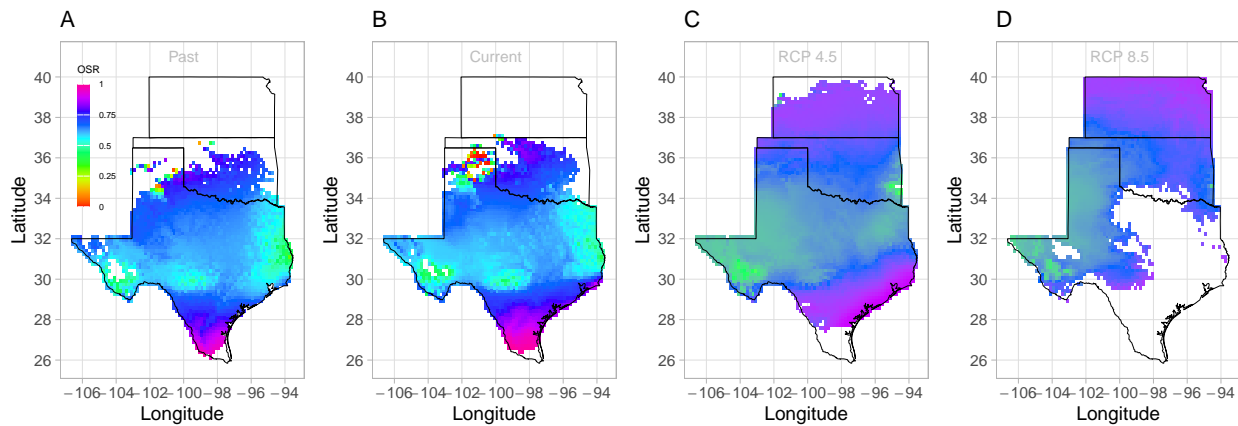


Figure S-21: Projection of Operational Sex Ratio (proportion of female panicle) over time (past, present, future) across species range. Future projections were based on the ACCESS model. The mean sex ratio for each time period is shown as vertical dashed line.

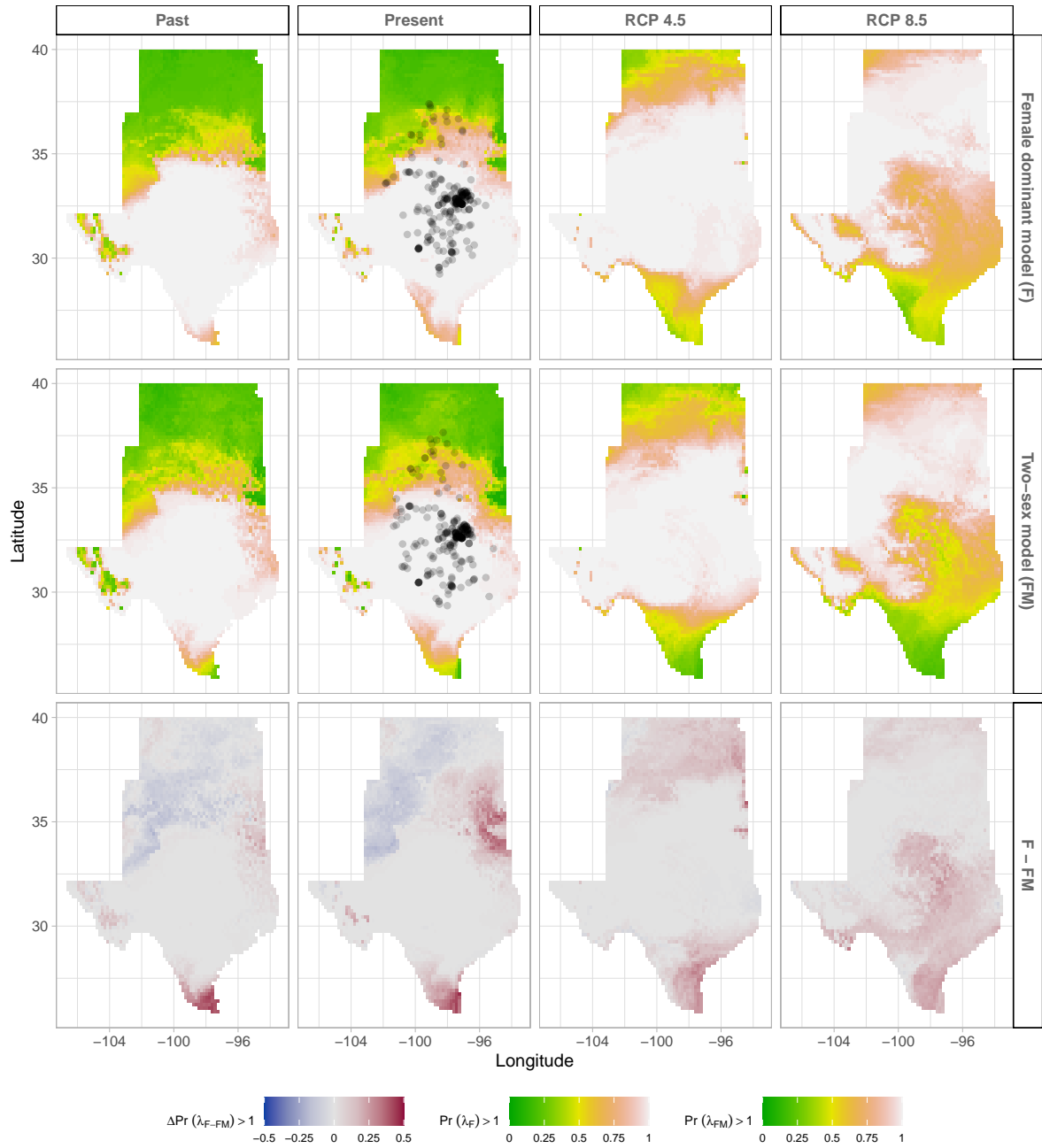


Figure S-22: Climate change favors range shift toward the North edge of the current range. (A) Past, (B) Current, (C and D) Future predicted range shift based on the predicted probabilities of self- sustaining populations, $\Pr(\lambda > 1)$, using the two-sex model that incorporates sex- specific demographic responses to climate with sex ratio dependent seed fertilization. (E) Past, (F) Current, (G and H) Future predicted range shift based on the predicted probabilities of self- sustaining populations, $\Pr(\lambda > 1)$, using the female dominant model. Future projections were based on the CESM1-BGC model. The black dots on panel B and F indicate all known presence points collected from GBIF from 1990 to 2019, which corresponds to the current condition in our prediction. The occurrences of GBIFs are distributed in with higher population fitness habitat $\Pr(\lambda > 1)$, confirming that our study approach can reasonably predict range shifts.

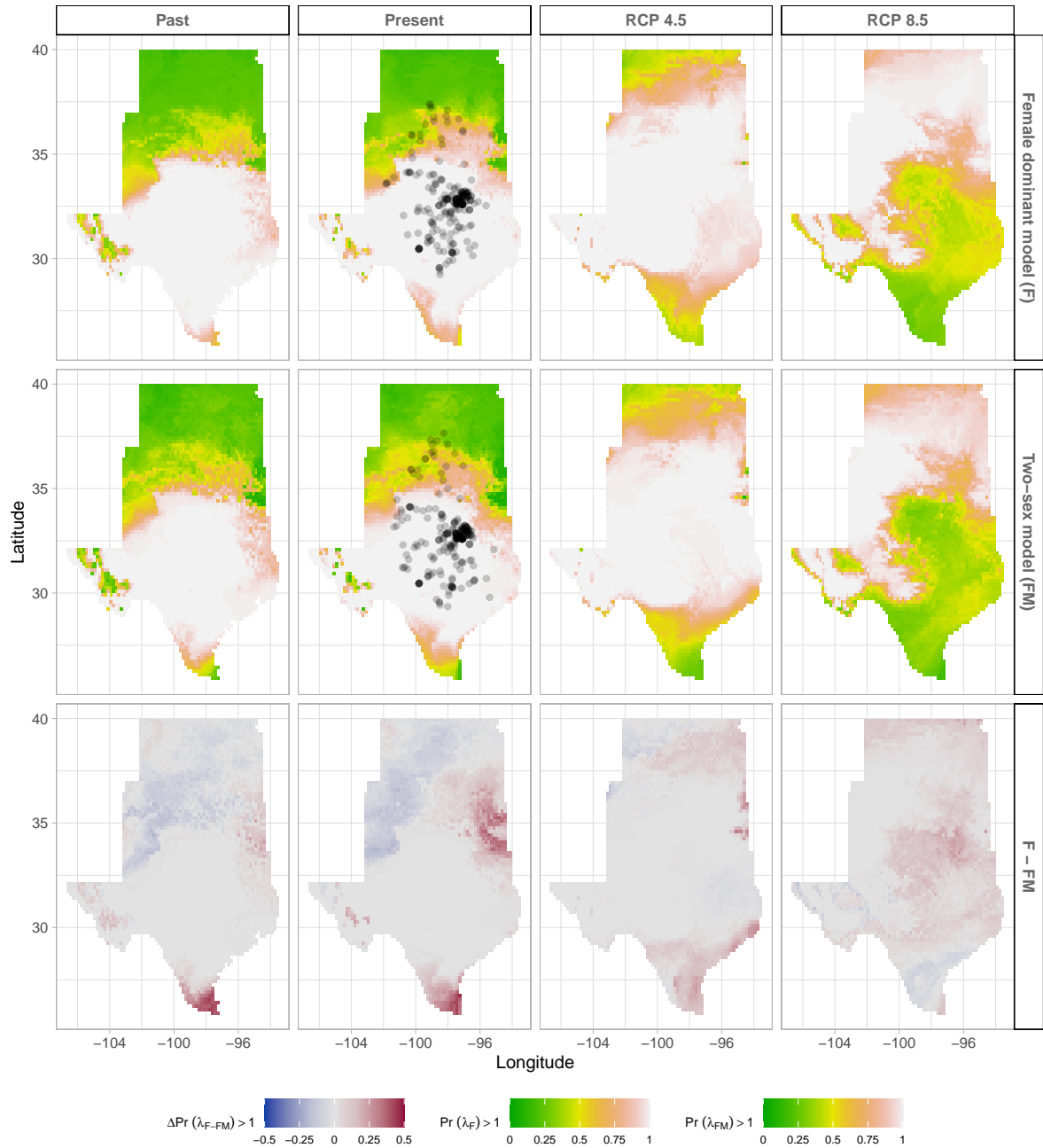


Figure S-23: Climate change favors range shift toward the North edge of the current range. (A) Past, (B) Current, (C and D) Future predicted range shift based on the predicted probabilities of self-sustaining populations, $\text{Pr}(\lambda > 1)$, using the two-sex model that incorporates sex-specific demographic responses to climate with sex ratio dependent seed fertilization. (E) Past, (F) Current, (G and H) Future predicted range shift based on the predicted probabilities of self-sustaining populations, $\text{Pr}(\lambda > 1)$, using the female dominant model. Future projections were based on the ACCESS model. The black dots on panel B and F indicate all known presence points collected from GBIF from 1990 to 2019, which corresponds to the current condition in our prediction. The occurrences of GBIFs are distributed in with higher population fitness habitat $\text{Pr}(\lambda > 1)$, confirming that our study approach can reasonably predict range shifts.

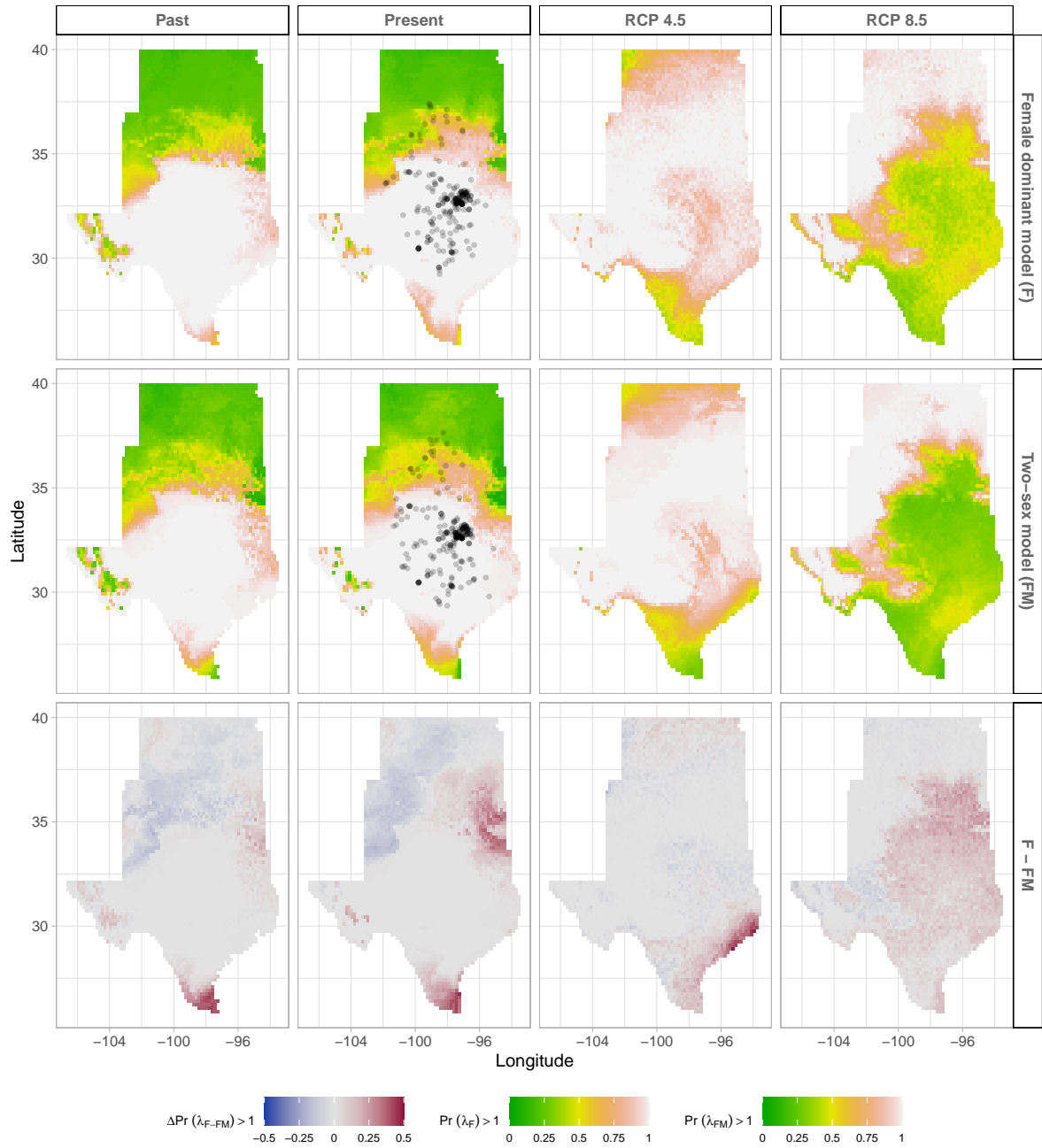


Figure S-24: Climate change favors range shift toward the North edge of the current range. (A) Past, (B) Current, (C and D) Future predicted range shift based on the predicted probabilities of self- sustaining populations, $\text{Pr}(\lambda > 1)$, using the two-sex model that incorporates sex- specific demographic responses to climate with sex ratio dependent seed fertilization. (E) Past, (F) Current, (G and H) Future predicted range shift based on the predicted probabilities of self- sustaining populations, $\text{Pr}(\lambda > 1)$, using the female dominant model. Future projections were based on the MIROC5 model. The black dots on panel B and F indicate all known presence points collected from GBIF from 1990 to 2019, which corresponds to the current condition in our prediction. The occurrences of GBIFs are distributed in with higher population fitness habitat $\text{Pr}(\lambda > 1)$, confirming that our study approach can reasonably predict range shifts.

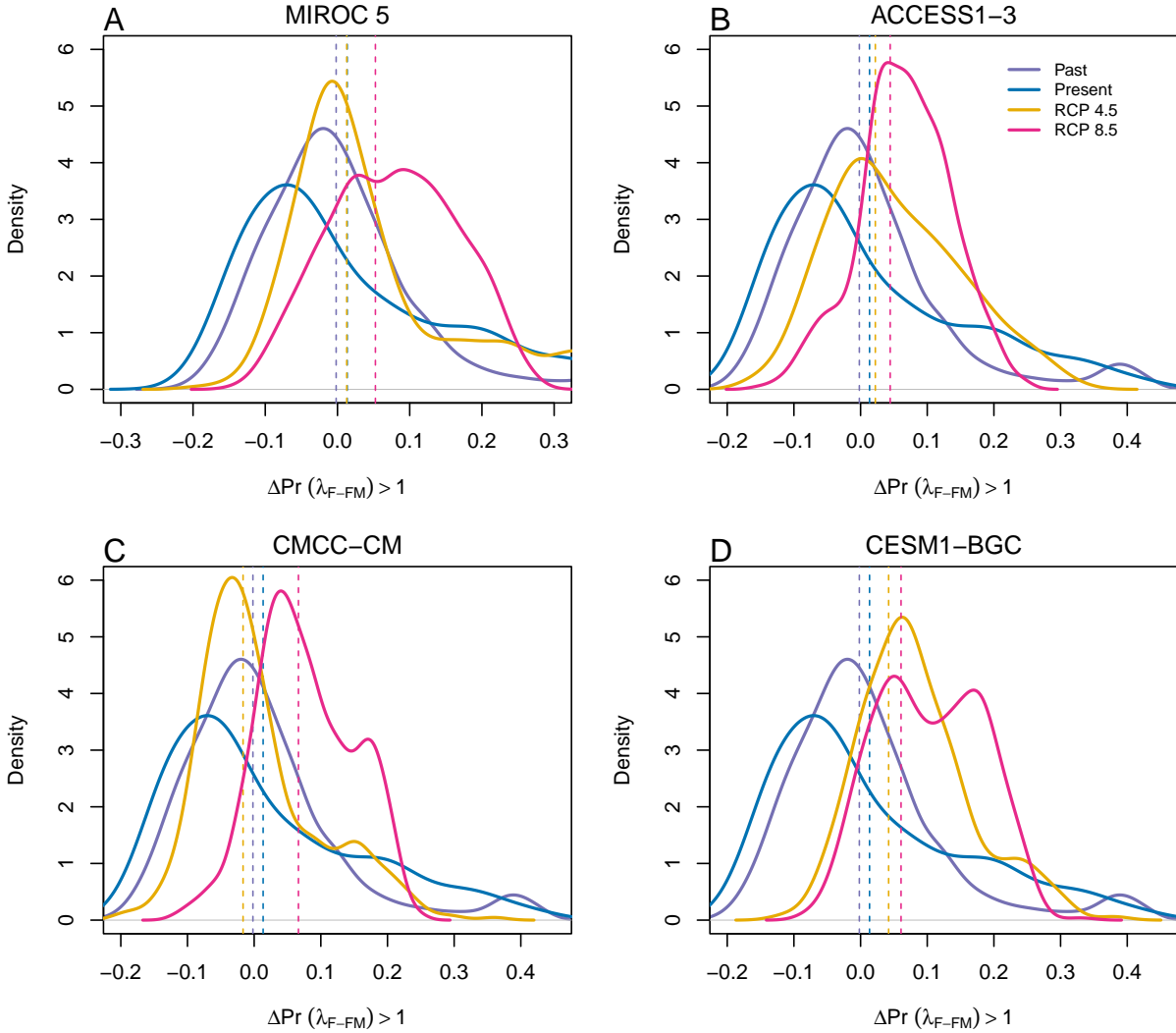


Figure S-25: Assessment of the statistical difference between the two-sex models and the female dominant model across and beyond species range for 4 GCMs. The means for each model are shown as vertical dashed lines.

691 S.2 Supporting Methods

692 S.2.1 Sex-specific demographic responses to climatic variation across 693 common garden sites

694 Vital rate models were fit with the same linear predictors for the expected value (μ) (Eq.S.1): All
695 vital rates were fit with second-degree polynomial functions to accommodate the possibility
696 of hump-shaped relationships (reduced demographic performance at both extremes). We
697 also included two-way interactions between sex and each climate driver and between
698 temperature and precipitation within each season, and a three-way interaction between sex,

699 temperature, and precipitation within each season. We modeled survival and flowering data
 700 with a Bernoulli distribution and the growth (tiller number) with a zero-truncated Poisson
 701 inverse Gaussian distribution. Fertility (panicle count conditional on flowering) was modeled
 702 as zero-truncated negative binomial. We used generic, weakly informative priors to fit
 703 coefficients for survival, growth, flowering models ($\beta \sim N(0, 1.5)$) and random effect variances
 704 ($\sigma \sim Gamma(\gamma(0.1, 0.1))$). We fit fertility model with also weakly informative priors for
 705 coefficients ($\beta \sim N(0, 0.15)$). Different priors were used for fertility because the panicle model
 706 has a large number of parameters relative to the amount of available data (subset of our data)
 707 and because these specific priors help prevent the model from overfitting. Each vital rate also
 708 includes normally distributed random effects for block-to-block variation ($\phi \sim N(0, \sigma_{block})$),
 709 site to site variation ($\nu \sim N(0, \sigma_{site})$), and source-to-source variation that is related to the
 710 genetic provenance of the transplants used to establish the common garden ($\rho \sim N(0, \sigma_{source})$).

$$\begin{aligned}
 \mu = & \beta_0 + \beta_1 size + \beta_2 sex + \beta_3 pptgrow + \beta_4 pptdorm + \beta_5 tempgrow + \beta_6 tempdorm \\
 & + \beta_7 pptgrow * sex + \beta_8 pptdorm * sex + \beta_9 tempgrow * sex + \beta_{10} tempdorm * sex \\
 & + \beta_{11} size * sex + \beta_{12} pptgrow * tempgrow + \beta_{13} pptdorm * tempdorm \\
 & + \beta_{14} pptgrow * tempgrow * sex + \beta_{15} pptdorm * tempdorm * sex + \beta_{16} pptgrow^2 \\
 & + \beta_{17} pptdorm^2 + \beta_{18} tempgrow^2 + \beta_{19} tempdorm^2 + \beta_{20} pptgrow^2 * sex \\
 & + \beta_{21} pptdorm^2 * sex + \beta_{22} tempgrow^2 * sex + \beta_{23} tempdorm^2 * sex + \phi + \rho + \nu
 \end{aligned} \tag{S.1}$$

712 where β_0 is the grand mean intercept, β_1 is the size dependent slopes. *size* was on a natural
 713 logarithm scale. $\beta_2 \dots \beta_{13}$ represent the climate dependent slopes. $\beta_{14} \dots \beta_{23}$ represent the sex-
 714 climate interaction slopes. *pptgrow* is the precipitation of the growing season, *tempgrow* is
 715 the temperature of the growing season, *pptdorm* is the precipitation of the dormant season,
 716 *tempdorm* is the temperature of the dormant season.

717 S.2.2 Sex ratio responses to climatic variation across common garden sites

718 To understand the impact of climatic variation across common garden sites on sex ratio, OSR
 719 and SR models using the same linear predictors for the expected value (ν)(Eq.S.2):

$$\begin{aligned}
 \nu = & \omega_0 + \omega_1 pptgrow + \omega_2 pptdorm + \omega_3 tempgrow + \omega_4 tempdorm + \\
 & \omega_5 pptgrow^2 + \omega_6 pptdorm^2 + \omega_7 tempgrow^2 + \omega_8 tempdorm^2 + \epsilon
 \end{aligned} \tag{S.2}$$

721 where OSR is the proportion of panicles that were female or proportion of female individuals
722 in the experimental populations, c is the climate. ω_0 is the intercept, $\omega_1, \dots, \omega_8$ are the climate
723 dependent slopes. ϵ is error term.

724 We modeled the OSR and SR data with a Bernoulli distribution and used non informative
725 priors for each coefficient ($\omega \sim N(0, 100)$).

726 S.2.3 Sex ratio experiment

727 To estimate the probability of seed viability, the germination rate and the effect of sex-ratio
728 variation on female reproductive success, we conducted a sex-ratio experiment at one site
729 near the center of the range to estimate the effect of sex-ratio variation on female reproductive
730 success. The details of the experiment are provided in Compagnoni et al. (2017) and Miller
731 and Compagnoni (2022b). Here we provide a summary of the experiment. We established
732 124 experimental populations in plots measuring $0.4 \times 0.4\text{m}$ and separated by at least 15m
733 from each other. We varied population density (1-48 plants/plot) and sex ratio (0%-100%
734 female) across the experimental populations, and we replicated 34 combinations of density
735 and sex ratio. We collected panicles from a subset of females in each plot and recorded the
736 number of seeds in each panicle. We assessed reproductive success (seeds fertilized) using
737 greenhouse-based germination and trazolium-based seed viability assays. Seed viability was
738 modeled with a binomial distribution where the probability of viability (v) was given by:

$$739 v = v_0 * (1 - OSR^\alpha) \quad (\text{S.3})$$

740 where OSR is the proportion of panicles that were female in the experimental populations.
741 α is the parameter that control for how viability declines with increasing female bias. Further,
742 germination rate was modeled using a binomial distribution to model the germination
743 data from greenhouse trials. Given that germination was conditional on seed viability, the
744 probability of success was given by the product $v * g$, where v is a function of OSR (Eq. S.3)
745 and g is assumed to be constant.